NASA TECHNICAL MEMORANDUM

DEVELOPMENT AND TESTING
OF ABLATIVE ROCKET ENGINE WITH
SELECTED 7.62-CENTIMETER (3.0 IN.)
DIAMETER THROAT INSERTS

by Jerry M. Winter, Donald A. Peterson,
Arthur M. Shinn, Jr., and Albert J. Pavli

Lewis Research Center
Cleveland, Ohio 44135

19960314 021

NATIONAL AERONAUTICS AND SPACE ADMINISTRATION • WASHINGTON, D. C. • JULY 1971

1. Report No. NASA TM X-2315	2. Government Accession No.	3. Recipient's Catalog No.
4. Title and Subtitle DEVELOPMENT AND TESTING OF ABLATIVE ROCKET ENGINE WITH SELECTED 7.62-CENTIMETER (3.0 IN.) DIAMETER THROAT INSERTS		5. Report Date July 1971
		6. Performing Organization Code
7. Author(s) Jerry M. Winter, Donald A. Peterson, Arthur M. Shinn, Jr., and Albert J. Pavli		8. Performing Organization Report No. E-6197
9. Performing Organization Name and Address Lewis Research Center National Aeronautics and Space Administration Cleveland, Ohio 44135		10. Work Unit No. 731-12
		11. Contract or Grant No.
12. Sponsoring Agency Name and Address National Aeronautics and Space Administration Washington, D. C. 20546		13. Type of Report and Period Covered Technical Memorandum
		14. Sponsoring Agency Code

15. Supplementary Notes

16. Abstract

Five injector configurations were designed and the performance evaluated in a nitrogen tetroxide - 50-percent blend of unsymmetrical dimethyl-hydrazine and hydrazine propellant rocket engine. A triplet injector modified for O/F zoning provided combustion efficiency of over 95 percent. Selected throat inserts (7.62 cm (3.0 in.) in diameter) were tested to demonstrate long-term firing duration and restart capability. The duty cycle chosen was an initial 300-second firing, five 20-second firings and a final 300-second firing. The best throat insert material tested was zirconia reinforced with tungsten-rhenium wire. Scale-up to larger throat sizes is discussed.

17. Key Words (Suggested by Author(s)) Earth-storable; Injectors; Rocket engine; Ablative; Throat insert	18. Distribution Statement Unclassified - unlimited		
19. Security Classif. (of this report) Unclassified	20. Security Classif. (of this page) Unclassified	21. No. of Pages 47	22. Price* $3.00

DEVELOPMENT AND TESTING OF ABLATIVE ROCKET ENGINE WITH SELECTED

7.62-CENTIMETER (3.0 IN.) DIAMETER THROAT INSERTS

by Jerry M. Winter, Donald A. Peterson, Arthur M. Shinn, Jr.,
and Albert J. Pavli

Lewis Research Center

SUMMARY

Development of the pressure fed engine included testing of five injector configurations with ablative thrust chambers. The best injector configuration was tested with eight hard throat inserts designed to prevent throat erosion.

Nominal design conditions were a chamber pressure of 100 psia and an oxidant to fuel mixture ratio of 2.0 using nitrogen tetroxide oxidizer with a 50 percent blend of unsymmetrical dimethyl hydrazine and hydrazine fuel. An arbitrary duty cycle of one 300-second firing, five 20-second firings, and one 300-second firing was selected to demonstrate long-term firing with restart capability.

The throat diameter of 7.62 centimeters (3.0 in.) provided a thrust of 4450 newtons (1000 lbf) with the expansion area ratio of 2.0 used at the sea-level test facility.

The injector developed for throat insert testing was a grid pattern using mutually perpendicular fuel-oxidant-fuel triplet elements. The outer elements of the injector were modified to be radially oriented with two fuel orifices on the outside, an oxidant orifice, and another fuel orifice on the inside. This provided reasonable ablative-insert compatibility with ηC^* efficiency of 95.3 percent theoretical equilibrium at a mixture ratio of 2.0.

Of the nine inserts tested, the best material combination was zirconia reinforced with tungsten-rhenium wires. An unsegmented insert of magnesia stabilized zirconia reinforced with 7-volume-percent, 0.005-centimeter (0.002-in.) diameter tungsten-rhenium wires, completed the chosen duty cycle with no throat erosion but with surface spallation and minor cracking. A segmented design using magnesia-calcia stabilized zirconia reinforced with 5-volume-percent, 0.0089-centimeter (0.0035-in.) diameter tungsten-rhenium wires, also completed the chosen duty cycle but with less cracking and less surface spallation than the unsegmented design.

These test results indicated that for large inserts, an optimized design approach would be segmenting to prevent gross structural failure and use of magnesia-calcia stabilized zirconia reinforced with 5-volume-percent, 0.0089-centimeter (0.0035-in.) diameter tungsten rhenium wires for reinforcement to minimize loss of material by surface spallation.

INTRODUCTION

Ablative thrust chambers are presently used in many important applications ranging in size from small reaction control engines to main propulsion systems. Many of these applications such as the Apollo Command and Lunar Module engines use earth storable propellants. Earth storable propellants such as nitrogen tetroxide with a 50 percent blend of unsymmetrical dimethyl hydrazine and hydrazine are attractive because they are easily stored as liquids in a near-earth environment and because they are hypergolic. Ablative thrust chambers are attractive because of their simplicity and reliability as well as adaptability to engine throttling.

Combining ablative thrust chambers with earth-storable propellants requires some compromises, however, particularly for long duration applications approaching 1000 seconds of engine operation. It has been shown (ref. 1) that throat erosion leads to a decrease in engine performance and much research has been aimed at preventing ablative throat erosion. Previous work (refs. 1 to 3) has established the best ablative materials and fabrication methods for use with earth-storable propellants. Because these materials are generally phenolic resins reinforced with silica, thrust chamber durability is limited by the melting point of the silica reinforcement (1780 to 2000 K or 3200° to 3600° R). Two methods are available for improvement in silica-phenolic ablative thrust chamber durability. One method would be to decrease the combustion gas temperature either by decreasing injector efficiency or by O/F zoning of the injector to provide a cooler boundary layer. Another approach intended to retain maximum performance for extended run durations, is to use a hard throat insert of erosion resistant material. Both of these methods require major design and development efforts if high performance is to be maintained.

The most successful throat inserts used with earth-storable propellants, have been restricted to small (3.05 cm or 1.2 in.) throat diameters (ref. 4). Only limited success has been achieved in the larger 19.8-centimeter (7.8-in.) diameter throat sizes of main liquid propulsion engines (refs. 5 and 6). The main objective of this program was to develop an ablative thrust chamber assembly for throat insert application in an intermediate size. The throat size chosen was 7.62 centimeters (3.0 in.) in diameter. It was felt that these inserts would represent reasonable scale-up for the successful concepts of 3.05-centimeter (1.2-in.) throat diameter (ref. 4). Larger diameter inserts such as 19.8-centimeter (7.8-in.) throat diameter would involve manufacturing difficulties and thus higher costs for this program. It was felt that a pressure fed engine of the size proposed (having 4450 N (1000 lbf) at sea level) might be applicable for unmanned exploration of the near planets. If the inserts were successful, further scale-up could be attempted with higher confidence than that derived from 3.05-centimeters (1.2-in.) throat diameter testing.

The program included the design and testing of two basic injector types with the goal of providing high performance, reasonable ablative compatibility, and long duration firing capability. Once these requirements were met, the throat inserts could be tested. Injector performance runs were made with heat-sink and water-cooled hardware. The nominal test conditions were a chamber pressure of 690 kilonewtons per square meter (100 psia) and an oxidant to fuel ratio of 2.0. A series of seven ablative thrust chambers was tested during the injector development phase. Materials were silica-phenolic combinations found superior in the testing of references 2 and 3. Eight throat inserts were then tested during the insert development phase. Materials selected were those which performed well in the 3.05-centimeter (1.2-in.) throat diameter size reported in reference 4. Economy and the ability to scale an insert-material design to large size were among other considerations in selecting materials for test. An arbitrary duty cycle of one 300-second firing, followed by five 20-second firings, and ending with a 300-second firing was chosen as an objective to demonstrate long duration and cyclic firing capability of the inserts.

SYMBOLS

A_t throat area, cm^2; $in.^2$

C^* characteristic exhaust velocity, m/sec; ft/sec

C_d flow coefficient, 0.991

g gravitational constant, $9.8 \ m/sec^2$; $32.174 \ ft/sec^2$

L^* characteristic chamber length, cm; in.

O/F oxidant-to-fuel mixture ratio

P_c chamber pressure measured at injector, kN/m^2; psia

R_i initial rocket throat radius, cm; in.

R_t throat radius at any time, cm; in.

V injection velocity, m/sec; ft/sec

Vol_c chamber volume, cm^3; $in.^3$

W_p propellant mass flow rate, kg/sec; lbm/sec

ΔP injector pressure drop, N/m^2; psi

ΔR_{eff} effective throat radius change, cm; in.

η efficiency

θ liquid jet spreading angle, deg

ρ density, kg/m^3; lbm/ft^3

φ momentum pressure loss correction (0.98 calculated by method of ref. 7)

Subscripts:

c   chamber

d   discharge

eff   effective

exp   experimental

f   fuel

i   initial

ox   oxidant

p   propellant

t   throat

theo   theoretical

FACILITY

Figure 1 is a photograph of the test facility. Shown is a thrust chamber installed in the horizontal thrust stand. Exhaust products were expelled from the nozzle at ambient pressure and then collected and water scrubbed before discharge into the air. The flow schematic of figure 2 illustrates the location of the measuring sensors.

Instrumentation

Chamber pressure measurements were made through a hole in the injector face using redundant strain gage bridge pressure transducers. Fuel and oxidant flow rates were each measured by venturi and turbine meters in series. Iron constantan thermocouples were used to measure propellant temperatures.
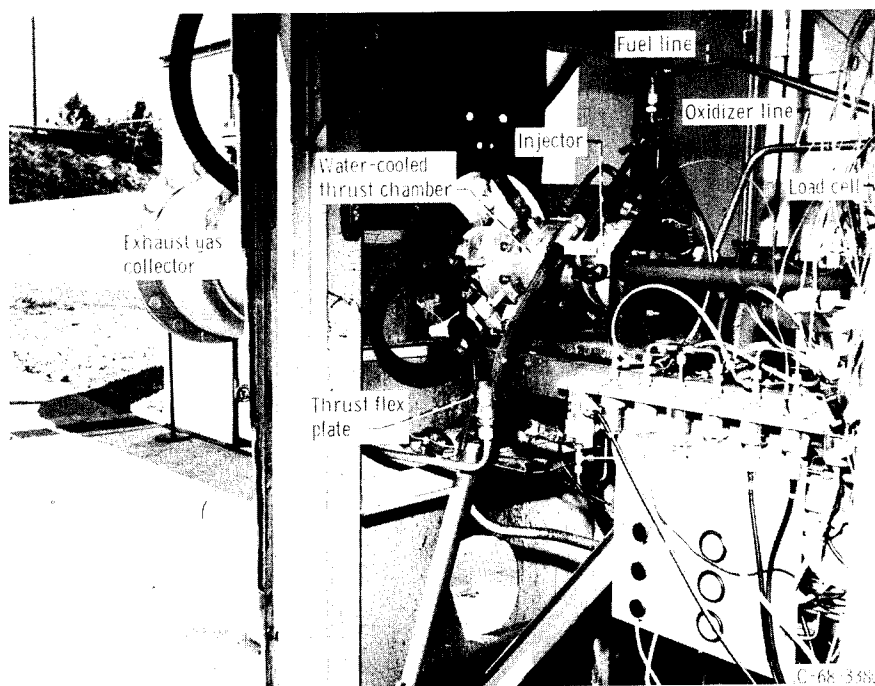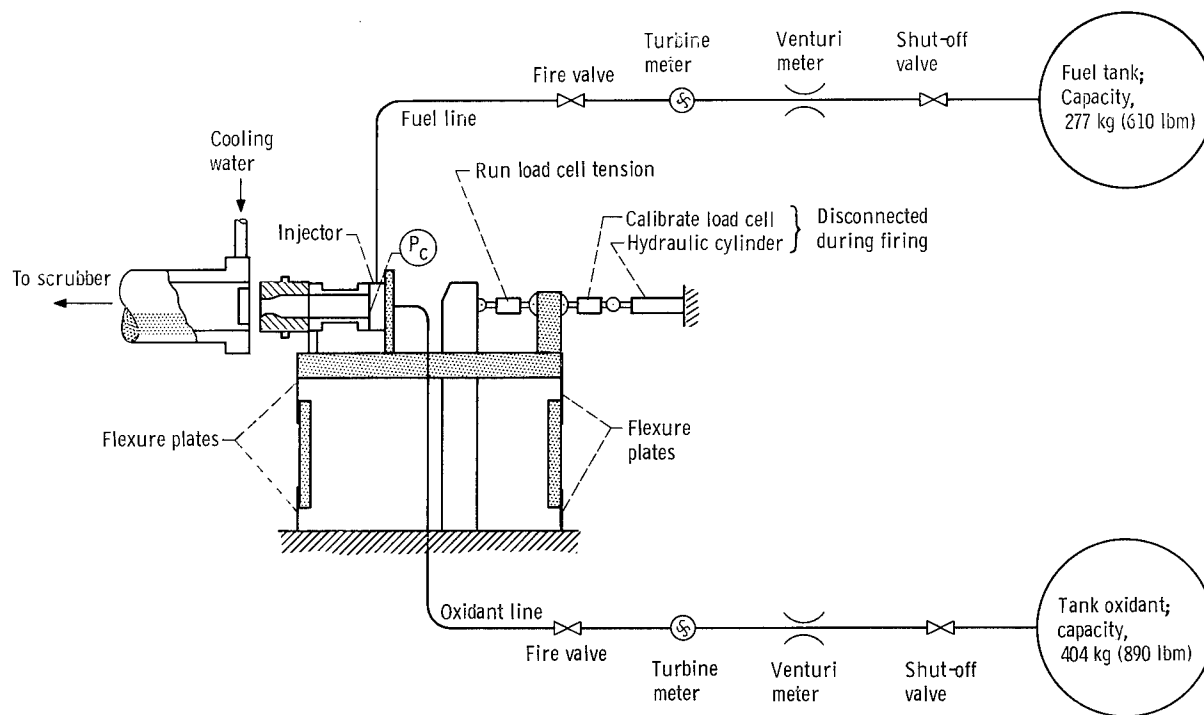
Figure 1. – Test facility.

Figure 2. – Flow system.

TABLE I. - INJECTOR DESCRIPTION

Injector Number	Type	Pattern	Oxidant holes Number	Oxidant Diameter cm	Oxidant Diameter in.	Fuel holes Number	Fuel Diameter cm	Fuel Diameter in.	Impingement Distance cm	Impingement Distance in.	Angle, deg	Design velocity ratio, V_{ox}/V_f	Design oxidant-to-fuel ratio, O/F
1	Triplet (fuel on ox)	Circular	61	0.109	0.043	122	0.053	0.021	1.421	0.560	40	0.60	2.00
2	Triplet (fuel on ox)	Grid	137	0.0889	0.035	274	0.046	0.018	1.310	0.516	30	0.67	2.00
2A	Triplet (low O/F zone on outside)	Grid	101 / 36	0.0889 / .0889	0.035 / .035	202 / 72	0.046 / .061	0.018 / .024	1.310	0.516	30	0.96	2.53 / 1.22
2B	Triplet (all outer elements radial)	Grid and radial	101 / 30 / 6	0.0889 / .0889 / .0889	0.035 / .035 / .035	202 / 60 / 12	0.046 / .057 / .061	0.018 / .0225 / .024	1.310	0.516	30	0.80	2.30 / 1.40 / 1.40
2C	Triplet and quadlet (all outer elements have three fuels on one ox)	Grid and radial	101 / 36	0.0889 / .0889	0.035 / .035	202 / 64 / 30 / 14	0.046 / .041 / .057 / .061	0.018 / .016 / .0225 / .024	1.310	0.516	30	0.86	2.45 / 1.31 / 1.31 / 1.31

Data Recording and Processing

Electrical outputs of 50 data channels were sampled at the rate of 2500 samples per second so that each output was recorded at 0.02-second intervals. Electrical signals were then digitized and recorded on magnetic tape. The data were converted to engineering quantities, and the appropriate calculations were made by a digital computer. Selected sensor outputs were also recorded continuously on strip charts and on oscillograph for system monitoring and control room processing.

THRUST CHAMBER ASSEMBLY

Injectors

Table I is a summary of the design values for all the injectors used in the program. The pattern and element detail of the injectors are shown in figures 3 to 5.

The basic injector designs were similar to those used in previous programs with the same propellants (refs. 5 to 7). Uniform injector face coverage, oxidant hole sizes 0.109-centimeter (0.043-in.) diameter or less, with oxidant to fuel velocity ratios of 0.6 to 0.7, had provided high combustion performance but not erosion-free ablative operation. The purpose here was to maintain high performance and combat ablative erosion by the installation of hard throat inserts.

Injector 1 had the elements arranged radially to provide spray fans parallel to the wall for ablative compatibility. Injector 2 had the elements mutually perpendicular for good mixing and high combustion performance. Modifications to injector 2 that evolved from testing will be discussed in a later section.

Thrust Chambers

The requirements of the program necessitated four different chamber designs. A heat sink thrust chamber (fig. 6) was designed to provide engine performance data for firing durations up to approximately 7 seconds. A contraction ratio of 3 and a characteristic length L^* of 37 was chosen. A photograph of the engine components is shown in figure 7.

A water-cooled chamber design, shown in figure 8, was intended for use in steady-state operation to measure performance and to check injector durability and also compatibility in combination with ablative components. A photograph of the water cooled thrust chamber components is shown in figure 9.

Diam, 2.94 (1.153);
six elements
equally spaced

Diam, 5.87 (2.301);
12 elements
equally spaced

Diam, 9.05 (3.56);
18 elements
equally spaced

Diam, 11.75 (4.62)
24 elements
equally spaced

Chamber diam;
13.20 (5.20)

Pattern symmetrical about centerline

1.42
(0.56)

40°

61 Oxidant holes;
diam, 0.889 (0.035)

122 fuel holes;
diam, 0.053 (0.021)
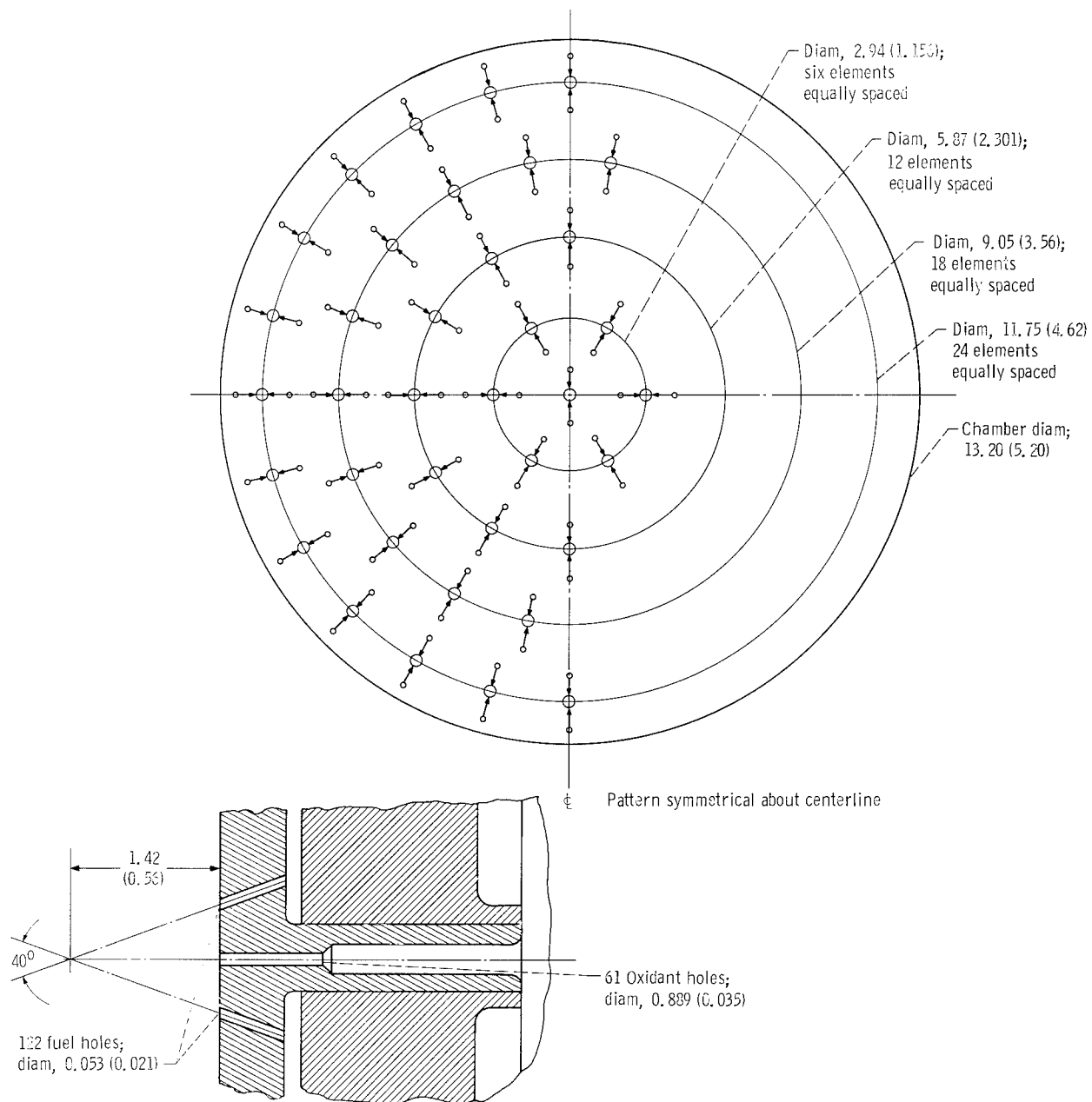
Element detail - scale 2/1

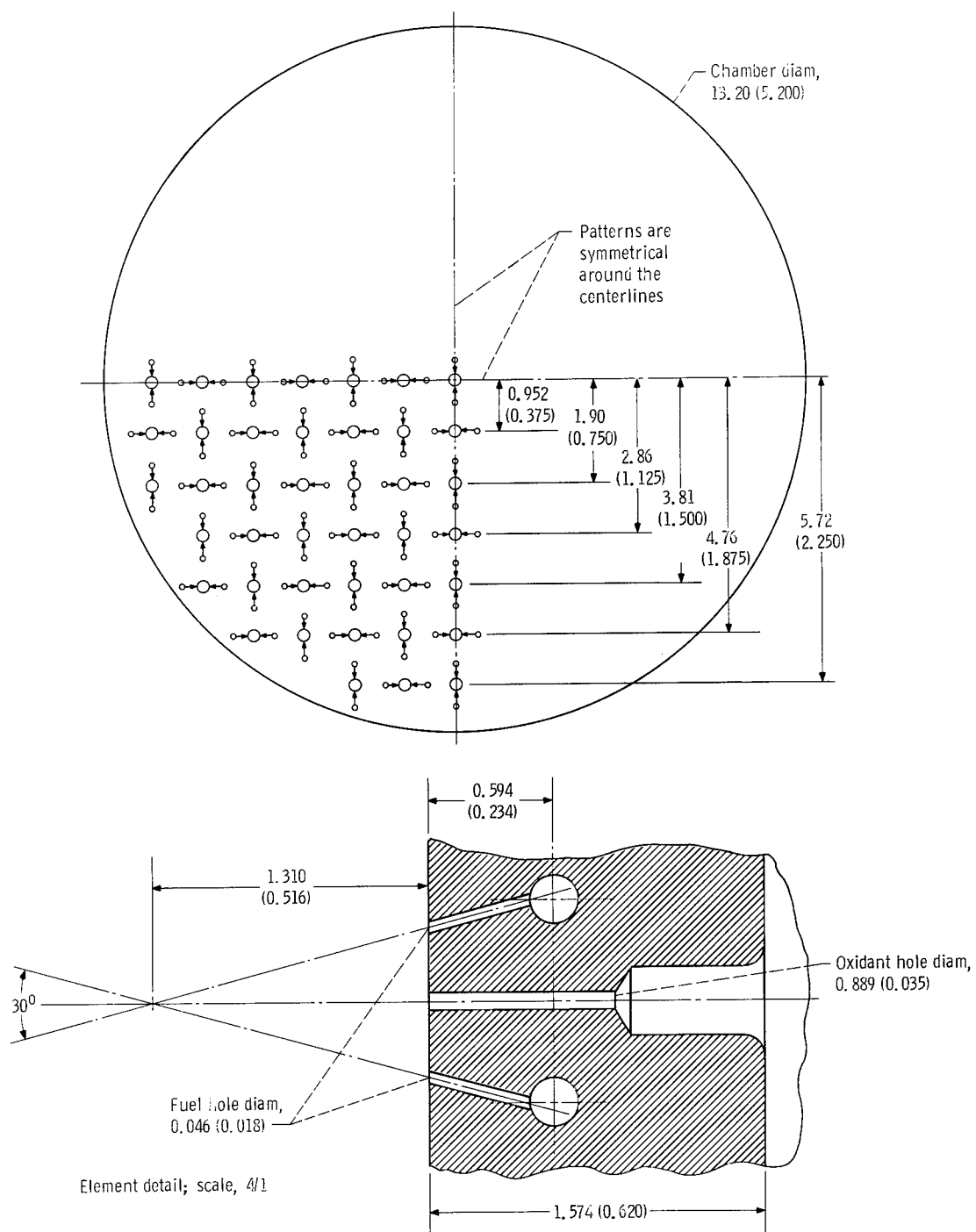Figure 3. - Injector 1. (All dimensions not otherwise noted are in centimeters (in.).)

8

Figure 4. – Injector 2. (All dimensions not otherwise noted are in centimeters (in.).)

9

Elements	Fuel hole diameter, cm (in.)
1, 9, 11, 19, 27, 29	0.061 (0.024)
Other numbered elements	.057 (.0225)

(a) Injector 2A. Fuel holes on elements 1 to 36 were enlarged to 0.061 centimeter (0.024-in.) diameter.
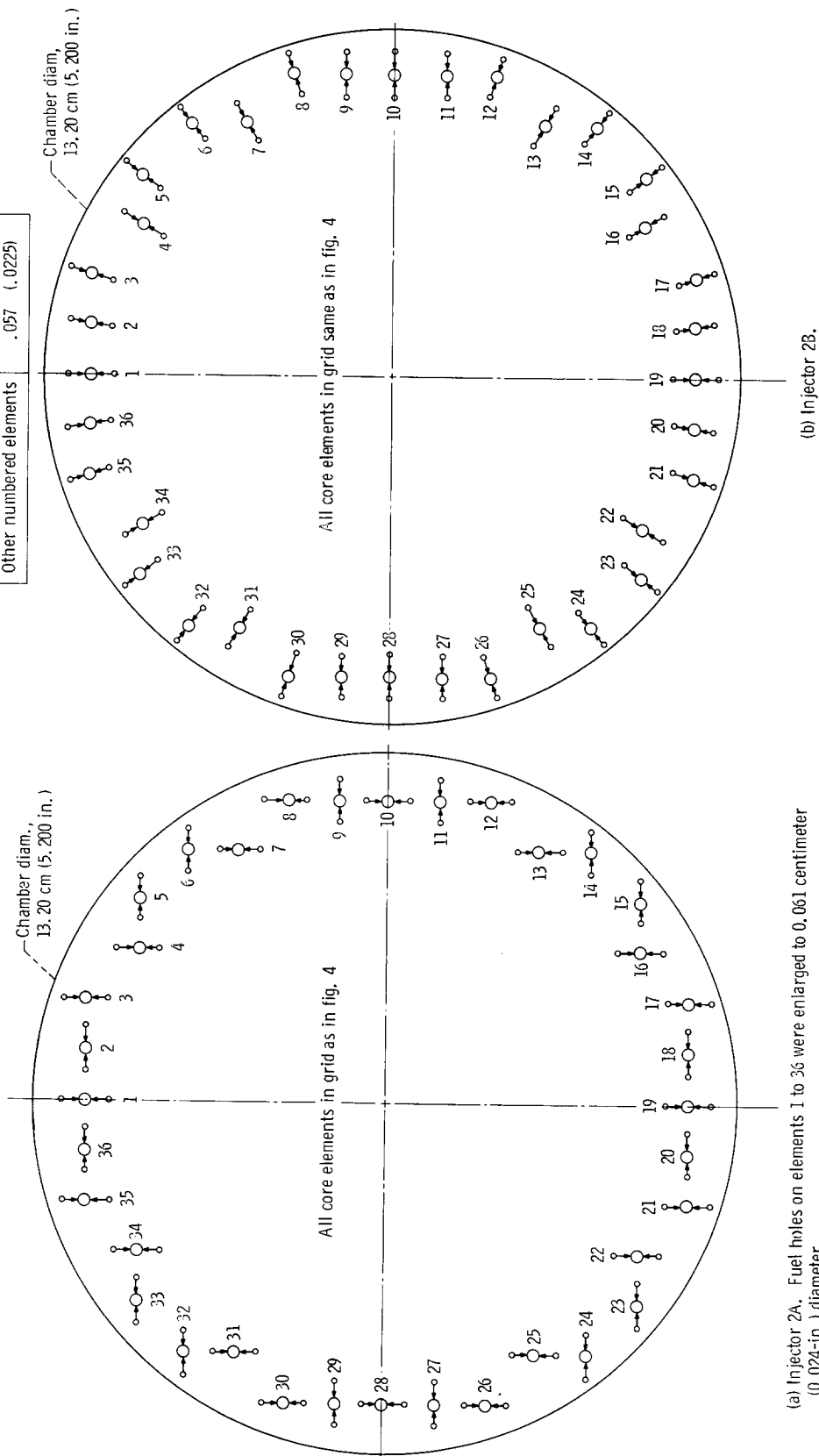
(b) Injector 2B.

Figure 5. – Modifications of injector 2.

All core elements in grid as on fig. 4

Chamber diam.,
13.20 cm (5.200 in.)
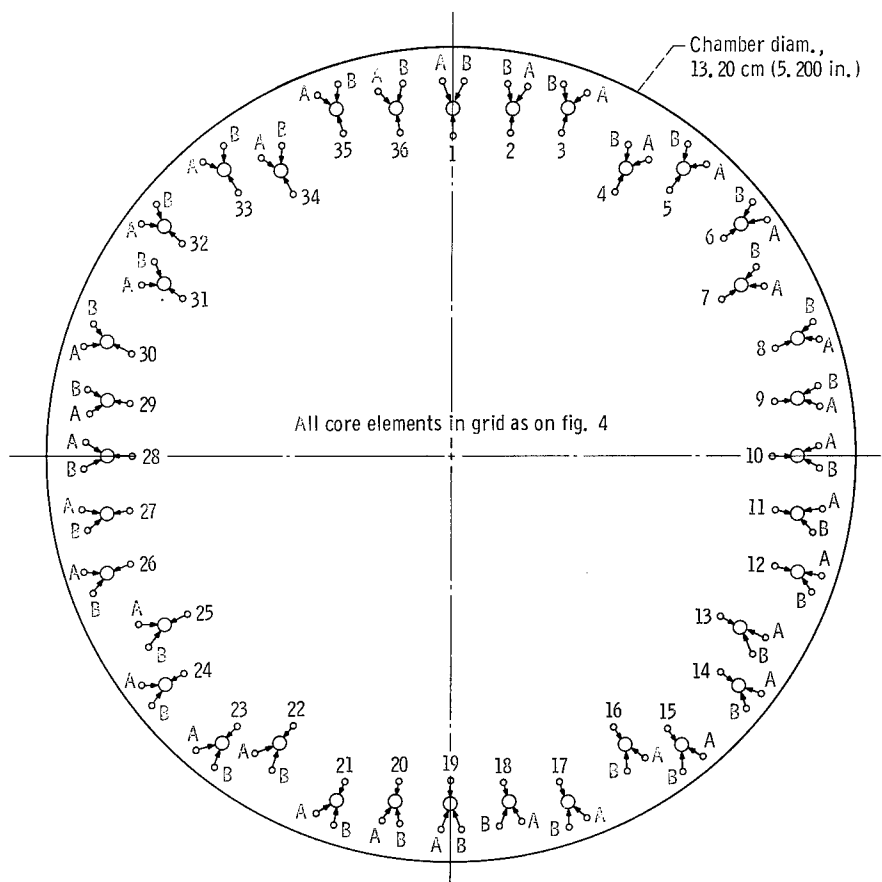
Elements	Outside (two)	Inside (one)
3, 17, 21, 35	0.061 (0.024)	0.057 (0.0225)
1, 9, 11, 19, 27, 29	.041 (.016)	.061 (.024)
All other numbered elements	.041 (.016)	.057 (.0225)

(c) Injector 2 C.

Figure 5. – Continued

11
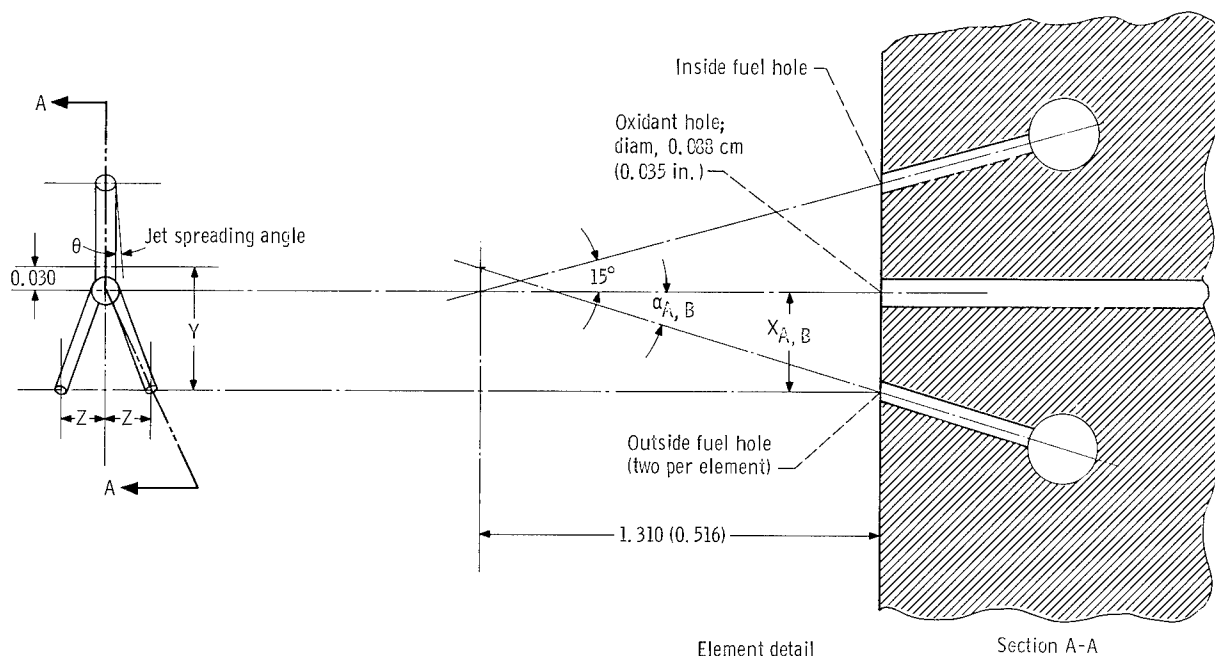
Element detail

Section A-A

A AND B NOTATION ON

Element	Y_A		Z_A		Y_B		Z_B		X_A		α_A	X_B		α_B
	cm	in.	cm	in.	cm	in.	cm	in.	cm	in.		cm	in.	
10, 28	0.401	0.1576	0.148	0.0585	0.401	0.1576	0.148	0.0585	0.434	0.1710	18° 20'	0.434	0.1710	18 20'
9, 11, 27, 29	.401	.1576	.148	.0585	.401	.1576	.148	.0585	.434	.1710	18° 20'	.434	.1710	18 20'
8, 12, 26, 30	.373	.1470	.138	.0545	.478	.1884	.177	.0696	.405	.1595	17° 10'	.517	.2035	21 30'
7, 13, 25, 31	.376	.1479	.139	.0549	.455	.1790	.168	.0662	.408	.1605	17° 20'	.492	.1935	20 30'
6, 14, 24, 32	.385	.1515	.143	.0563	.416	.1638	.155	.0610	.418	.1645	17° 40'	.454	.1785	19 0'
5, 15, 23, 33	.416	.1638	.155	.0610	.385	.1515	.143	.0563	.454	.1785	19° 0'	.418	.1645	17 40'
4, 16, 22, 34	.455	.1790	.168	.0662	.376	.1419	.139	.0549	.492	.1935	20° 30'	.408	.1605	17 20'
3, 17, 21, 35	.422	.1663	.154	.0605	Existing		Existing		.450	.1770	19° 0'	.352	.1385	15 0'
2, 18, 20, 36	.433	.1705	.160	.0631	.381	.1502	.142	.0558	.469	.1845	19° 40'	.414	.1630	17 30'
1, 19	.401	.1576	.148	.0585	.401	.1576	.148	.0585	.434	.1710	18° 20'	.434	.1710	18 20'

(d)

Figure 5. - Concluded.

(a) Chamber diameter, 13.2 centimeter (5.20 in.)

(b) Nozzle throat diameter, 7.62 centimeters (3.0 in.).

CD-10474-33
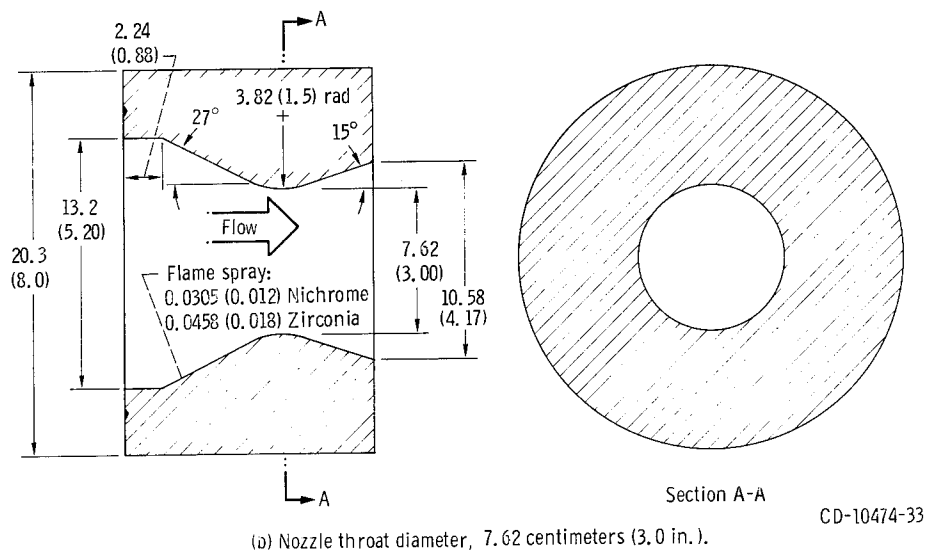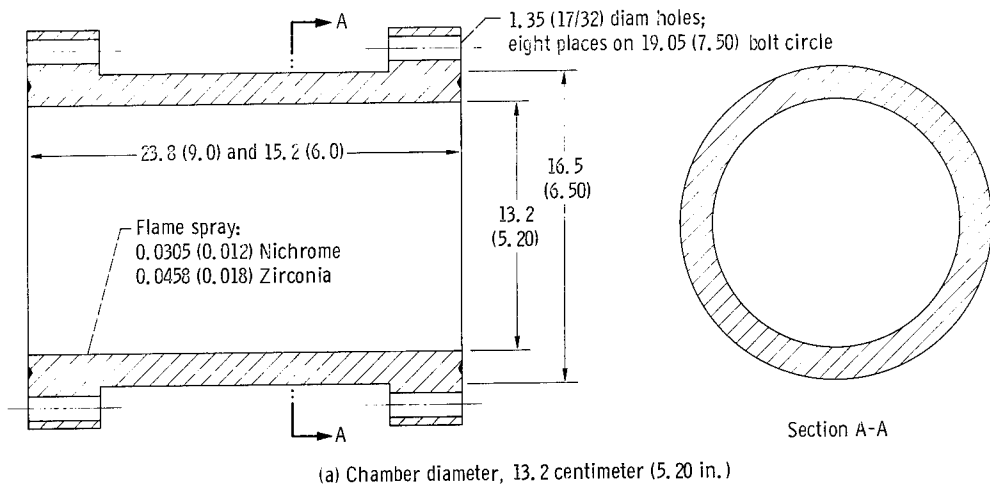
Figure 6. - Heat sink configuration. Material, mild steel. (All linear dimensions are in centimeters (in.).)
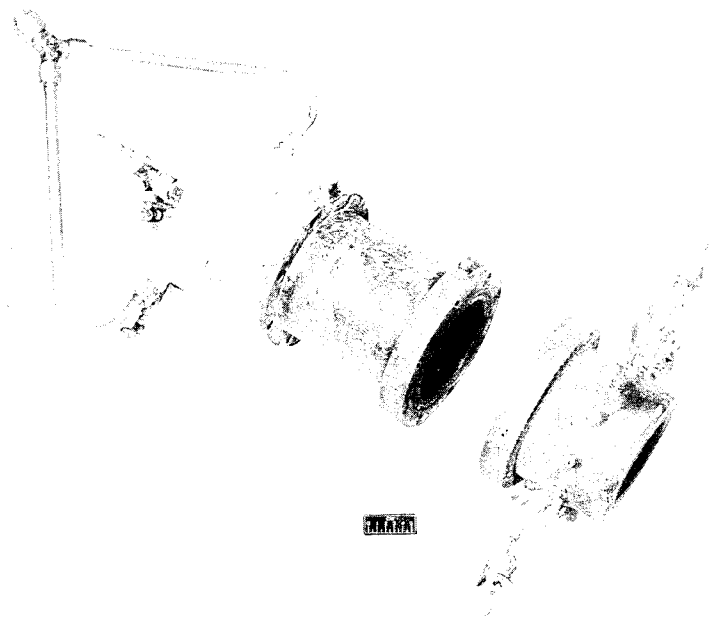
Figure 7. - Thrust chamber assembly: heat sink chamber and nozzle.
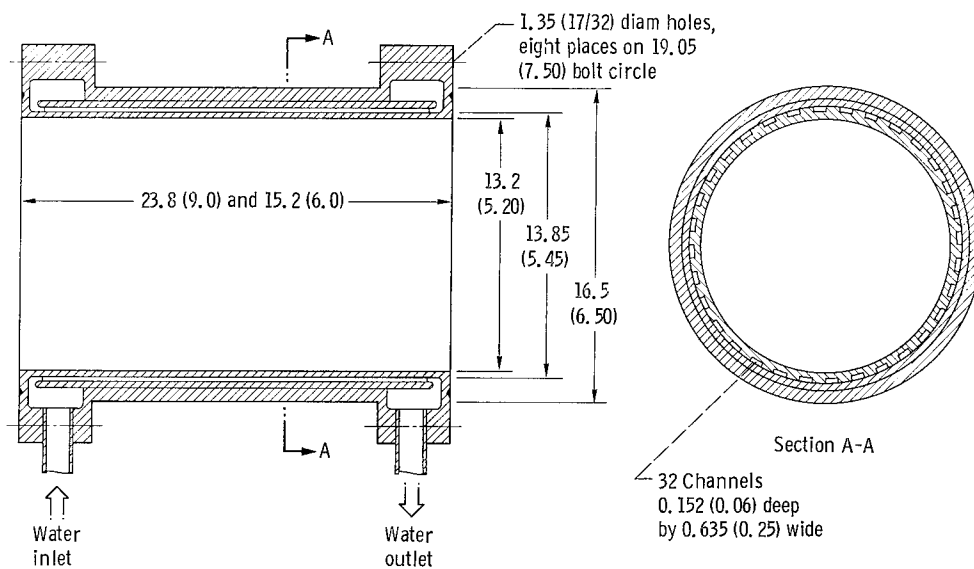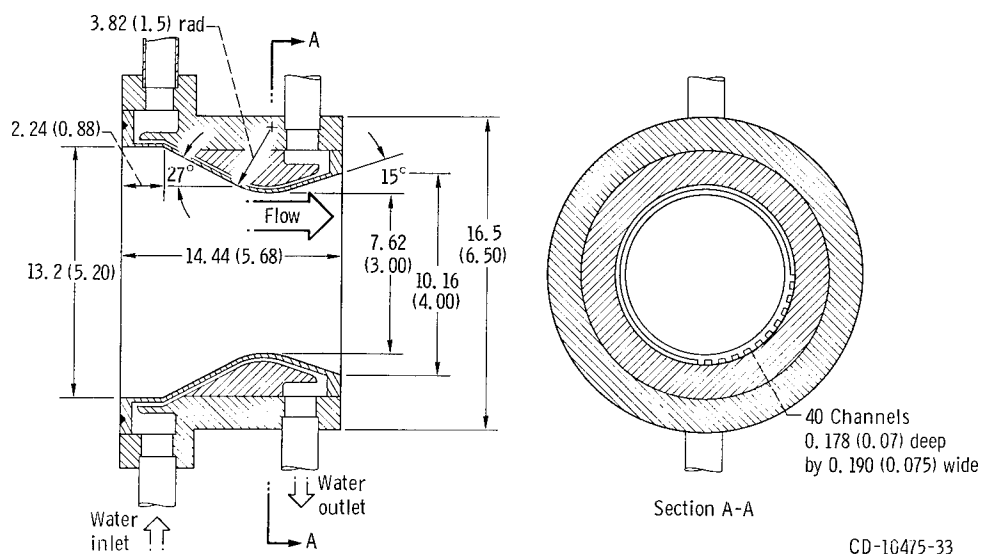
1.35 (17/32) diam holes,
eight places on 19.05
(7.50) bolt circle

23.8 (9.0) and 15.2 (6.0)

13.2
(5.20)

13.85
(5.45)

16.5
(6.50)

Section A-A

32 Channels
0.152 (0.06) deep
by 0.635 (0.25) wide

Water
inlet

Water
outlet

(a) Chamber diameter, 5.20 inches (13.2 cm).

3.82 (1.5) rad

2.24 (0.88)

27°

Flow

15°

7.62
(3.00)

16.5
(6.50)

13.2 (5.20)

14.44 (5.68)

10.16
(4.00)

40 Channels
0.178 (0.07) deep
by 0.190 (0.075) wide

Section A-A

CD-10475-33

Water
outlet

Water
inlet

(b) Nozzle throat diameter, 7.62 centimeters (3.0 in.).

Figure 8. – Water-cooled configuration. Material, 5083 aluminum. (All linear dimensions are in centimeters (in.).)

15
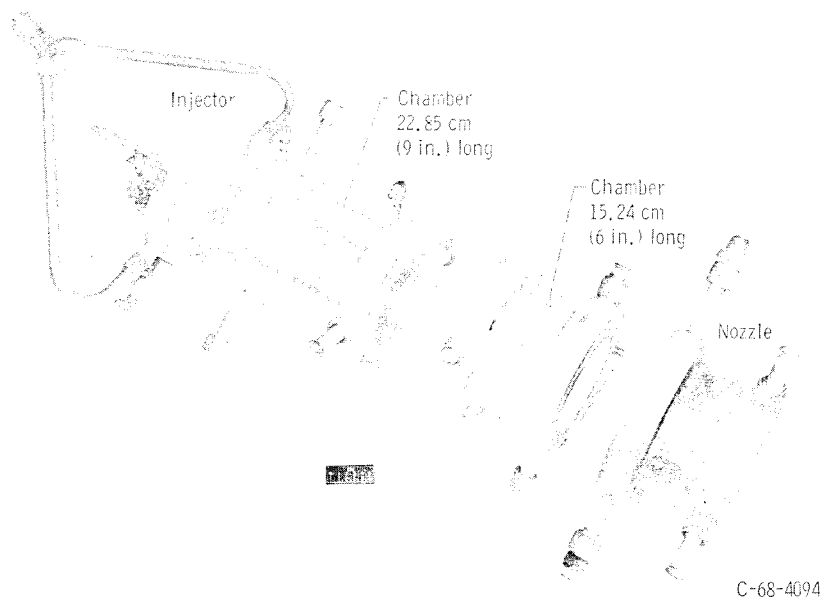
Figure 9. - Thrust chamber assembly; water-cooled chamber and nozzle.

For long duration firings, up to 1000 seconds, a silica/phenolic ablative thrust chamber was designed (fig. 10). The ablative chamber was necessary in order to evaluate the effect of injector modification on the erosion characteristics of the chamber wall.

The basic chamber design used to test the throat inserts is shown in figure 11(a). Figures 11(b) and (c) detail the throat insert design used for the segmented BeO and segmented reinforced zirconia concepts. A JTA graphite chamber liner was used where necessary to prevent excessive ablative chamber erosion.

An exit angle of 18° was chosen in the insert design instead of the usual 15° to reduce insert wall thickness and prevent cracking at the trailing edge. The standard 15° exit angle was chosen for all nozzles used to measure injector performance, however. Figure 12 is a photograph of the water-cooled chamber and ablative insert combination used to test the segmented designs (see figs. 11(b) and (c)).

16
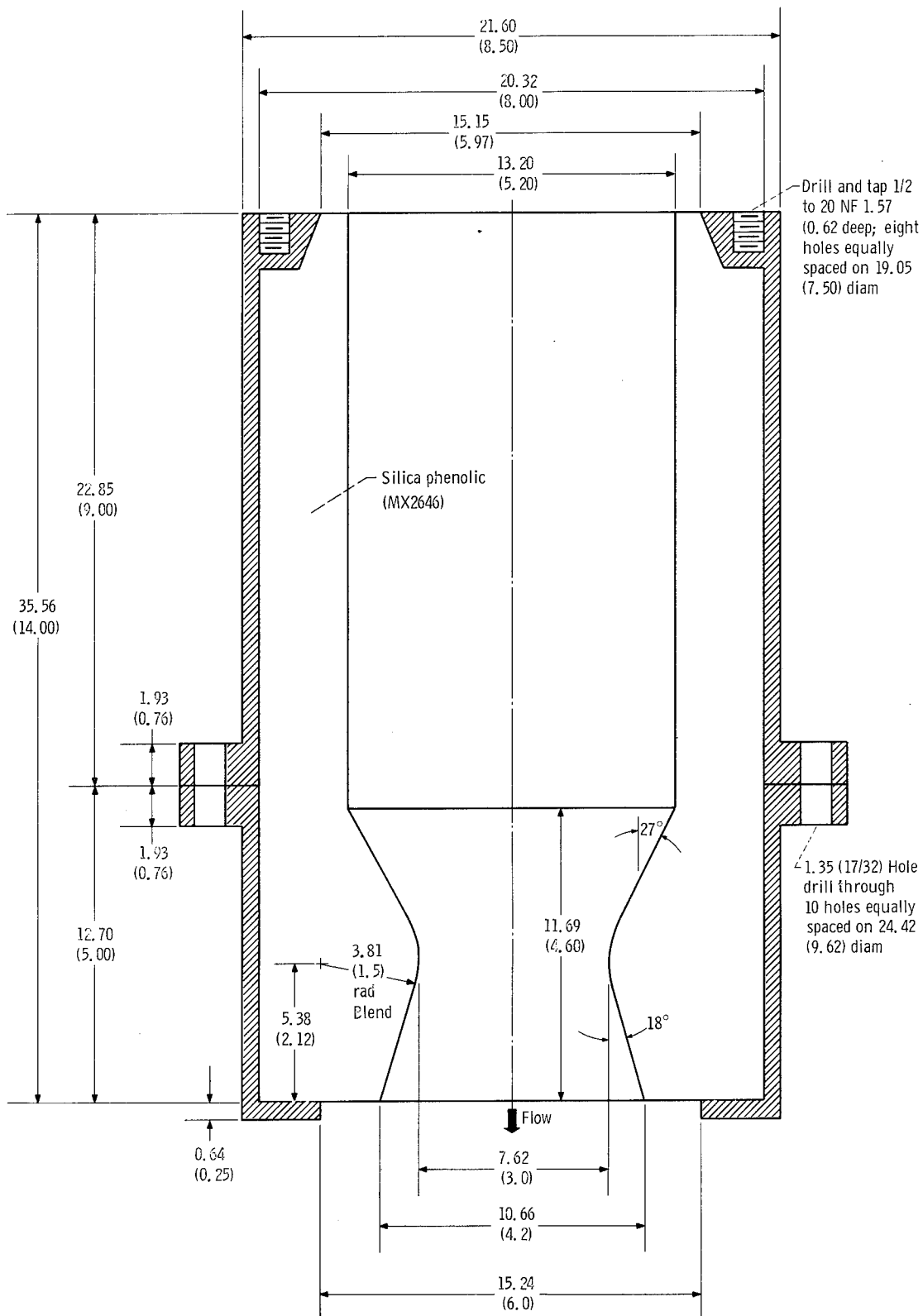
Figure 10. – Ablative thrust chamber. (All linear dimensions are in centimeters (in.).)
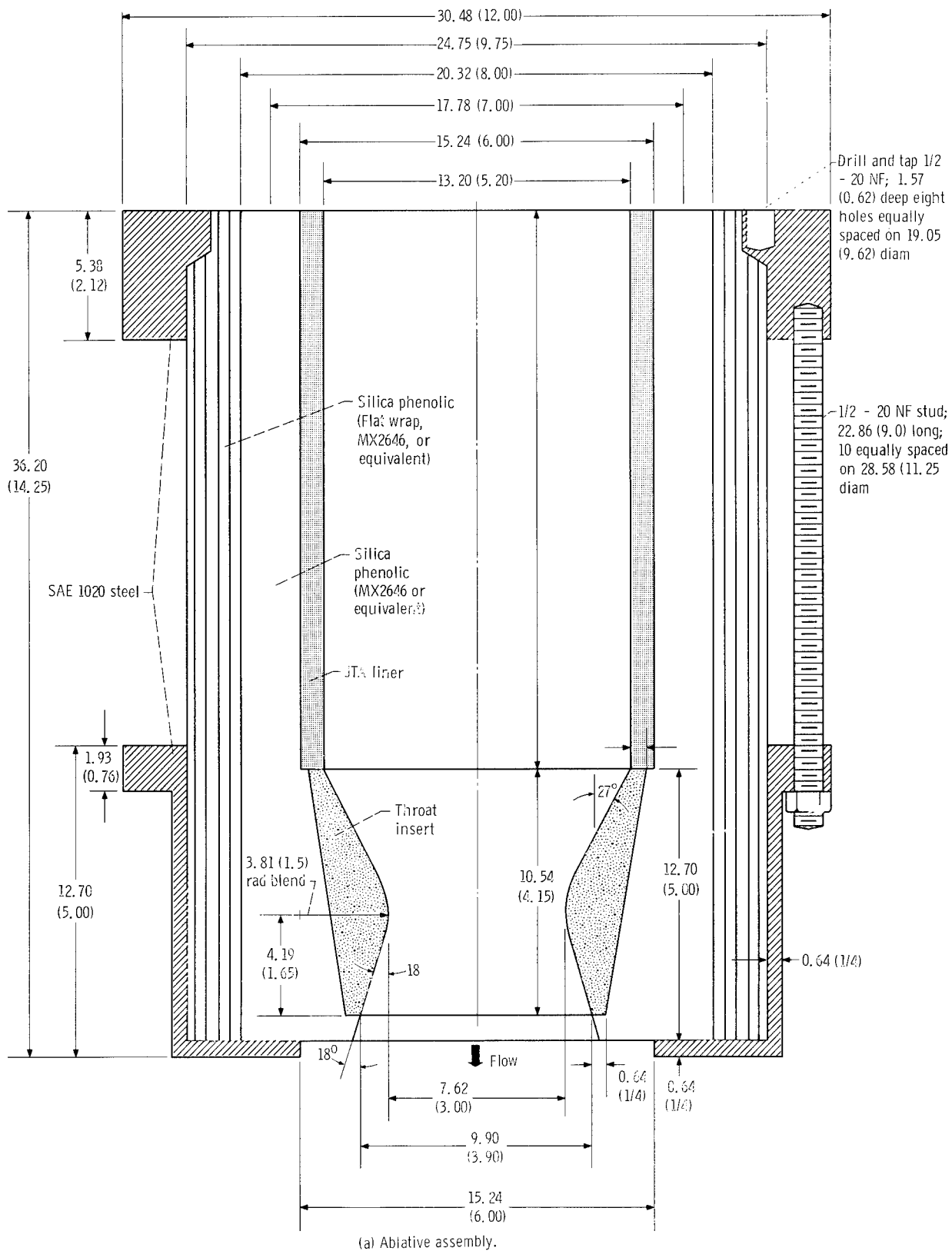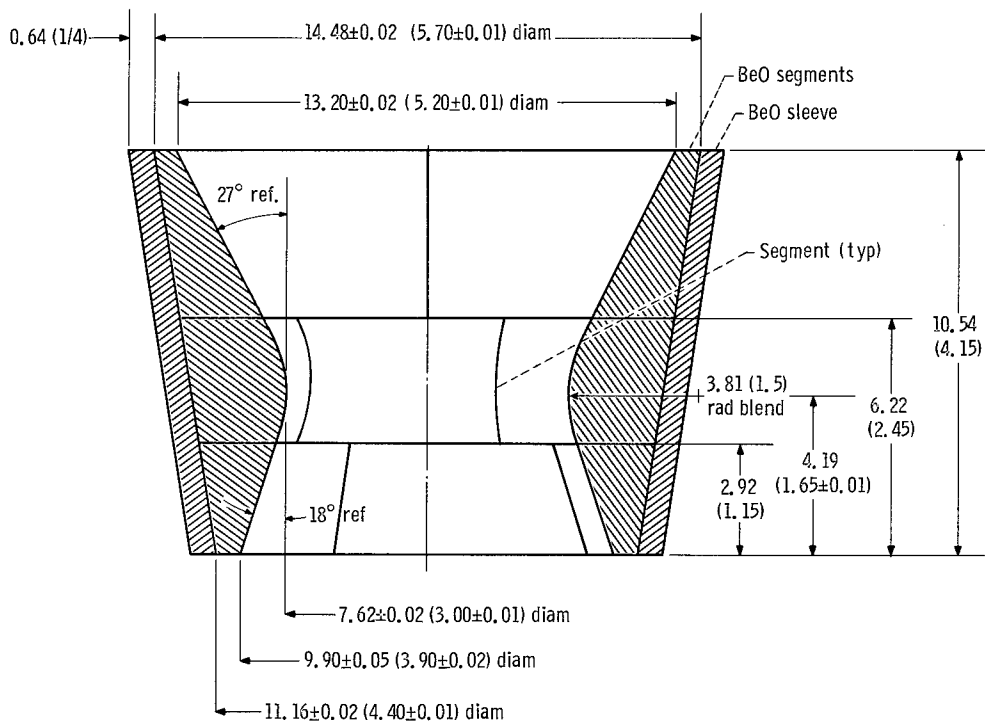
Figure 11. – Throat insert designs. (All linear dimensions are in centimeters (in.).)

Labels within figure:

- 30.48 (12.00)
- 24.75 (9.75)
- 20.32 (8.00)
- 17.78 (7.00)
- 15.24 (6.00)
- 13.20 (5.20)
- 5.38 (2.12)
- 36.20 (14.25)
- 1.93 (0.76)
- 12.70 (5.00)
- SAE 1020 steel
- Silica phenolic (Flat wrap, MX2646, or equivalent)
- Silica phenolic (MX2646 or equivalent)
- JTA liner
- Throat insert
- 3.81 (1.5) rad blend
- 4.19 (1.65)
- 18
- 27°
- 10.54 (4.15)
- 12.70 (5.00)
- 0.64 (1/4)
- Drill and tap 1/2 - 20 NF; 1.57 (0.62) deep eight holes equally spaced on 19.05 (9.62) diam
- 1/2 - 20 NF stud; 22.86 (9.0) long; 10 equally spaced on 28.58 (11.25) diam
- 18°
- Flow
- 7.62 (3.00)
- 0.64 (1/4)
- 0.64 (1/4)
- 9.90 (3.90)
- 15.24 (6.00)

(a) Ablative assembly.

18

0. 64 (1/4)

14. 48±0. 02 (5. 70±0. 01) diam

13. 20±0. 02 (5. 20±0. 01) diam

BeO segments

BeO sleeve

27° ref.

Segment (typ)

10. 54
(4. 15)

3. 81 (1. 5)
rad blend

6. 22
(2. 45)

4. 19

2. 92   (1. 65±0. 01)
(1. 15)

18° ref

7. 62±0. 02 (3. 00±0. 01) diam

9. 90±0. 05 (3. 90±0. 02) diam

11. 16±0. 02 (4. 40±0. 01) diam

(b) Segmented beryllium oxide (BeO) insert design. There are three axial segments composed of three 120° circumferential segments.

Figure 11. - Continued.

15.74+0.038 (6.20+0.015) diam
14.96 (5.70) diam
13.20±0.025 (5.20±0.010) diam

8° 54' ref.

Four radial segments;
90° joints staggered
30°/60° apart

0.010±0.005
(0.004±0.002)
Bond joint
(typical)

Segment (typical)

4.19±0.025
1.650±0.010

27° ref.

3.81 (1.5)
rad blend

4.19±0.025
(1.650±0.010)

2.910±0.013
(1.145±0.005)

18° ref.

3.018±0.013
(1.187+0.005)

7.620±0.025
(3.000±0.010) diam
9.900±0.025 (3.900±0.010) diam
11.160 (4.400) diam
12.45+0.038 (4.900+0.015) diam

(c) Segmented reinforced zirconia (ZrO$_2$) throat insert.

Figure 11. - Concluded.

C-68-4253

Figure 12. - Thrust chamber assembly: water-cooled chamber with throat insert ablative.

PROCEDURE

Engine Operation and Control

Before each firing, the propellant tanks were pressurized with nitrogen gas. Fire valve openings were automatically sequenced to provide an oxidant lead of approximately 0.1 second. Individual automatic closed-loop controllers were used to maintain a constant chamber pressure and oxidant-to-fuel ratio. The run duration was controlled by an automatic timer. An automatic cutoff was used to terminate any firing when the throat area increase exceeded 25 percent. Emergency shutdowns were made manually if gas leakage or excessive erosion rates were noted.

Throat Measurements

New ablative and throat insert diameters were measured with a micrometer. After erosion or surface roughening, photographs were taken of the throat plane. The enlarged photographs were measured with a planimeter to obtain throat area after firing, and the areas were converted to an effective radius.

The throat radius change was also calculated during each firing from instantaneous values of chamber pressure and weight flow.

Calculations

(1) Propellant injection velocity ratio:

$$\frac{V_{ox}}{V_f} = \sqrt{\frac{\Delta P_{ox}\rho_f}{\Delta P_f \rho_{ox}}}$$

(2) Characteristic exhaust velocity efficiency (no corrections were made due to heat losses):

$$\eta C^* = \frac{C^*_{exp}}{C^*_{theo}}$$

where C^*_{theo} is the theoretical one-dimensional shifting equilibrium characteristic velocity and

$$C^*_{exp} = \frac{\varphi P_c C_d A_{tg}}{W_p}$$

(3) Effective throat radius change:

$$R_t = \sqrt{\frac{W_p \eta C^*_{theo}}{\pi g \varphi P_c C_d}}$$

$$\Delta R_{eff} = R_i - R_t$$

(4) Characteristic chamber length:

$$L^* = \frac{Vol_c}{A_t}$$

RESULTS AND DISCUSSION

One of the major problems associated with development of ablative thrust chambers has been achieving a satisfactory compromise between injector performance and ablative material compatibility. Ablative silica-phenolic materials generally can provide satisfactory long-term erosion resistance if ηC^* values of approximately 90 percent are acceptable. The objective of this report was to develop throat inserts for long term erosion resistance with high performance injectors (above 95 percent ηC^*) where ablatives alone may be unsatisfactory. In this investigation, injector performance was first evaluated and then ablative compatibility was determined. The best injector was then used for insert evaluation.

Injector Development for Thrust Chamber Compatibility

Two basic injector designs were first tested with heat-sink thrust chambers to measure characteristic exhaust velocity efficiency. Injector 1 (fig. 3) consisted of fuel-oxidant-fuel triplets, radially oriented and arranged in a circular pattern. Element spacing provided uniform coverage of the entire chamber area. The design was based on a
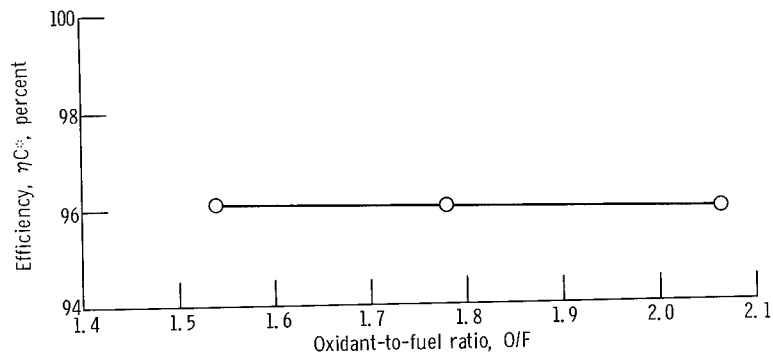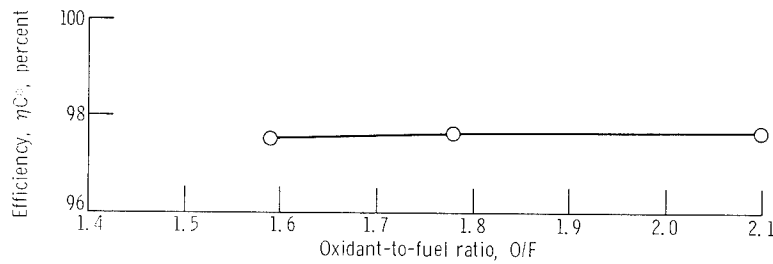
Figure 13. - Injector 1 combustion performance.
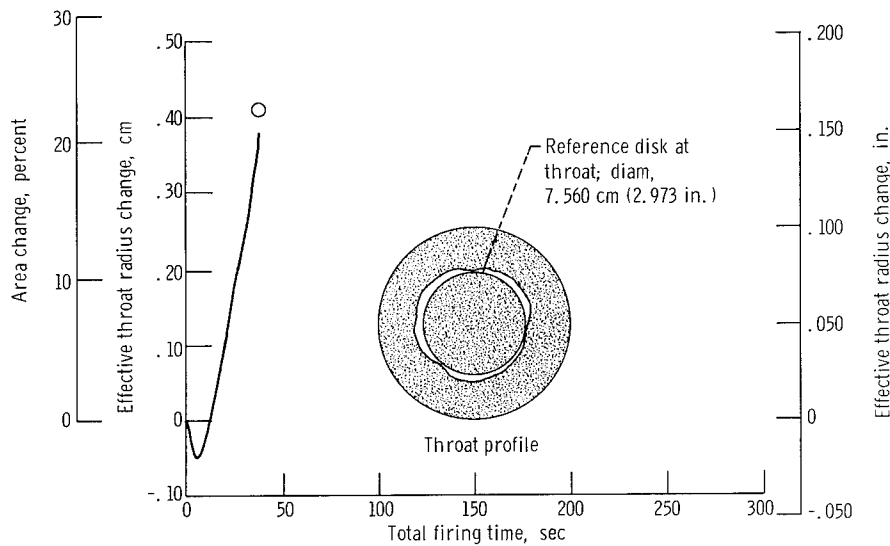
Figure 14. - Ablative erosion of silica phenolic (MX2646) chamber nozzle. Injector 1.

V_{ox}/V_{fuel} ratio of 0.60 similar to injectors of references 1 and 3.

Seven-second firing durations were used to ensure steady-state operation. The efficiency measured for injector 1 (a circular pattern triplet) is shown in figure 13. Since the performance was above the goal of 95 percent C^*, the injector was tested with an ablative chamber nozzle of MX2646 silica-phenolic material. The resulting erosion and post-test throat plane profile are given in figure 14. Steady-state erosion rate was very high and some gouging was evident.

In hopes of getting higher combustion performance with reduced ablative gouging, injector 2 was tested. The work of reference 5 indicated that higher performance was available with mutually perpendicular elements using smaller thrust per element. The oxidant-to-fuel velocity ratio of 0.66 used was similar to the velocity ratio for the injectors of references 1 and 3.

Figure 15. - Injector 2 combustor performance.
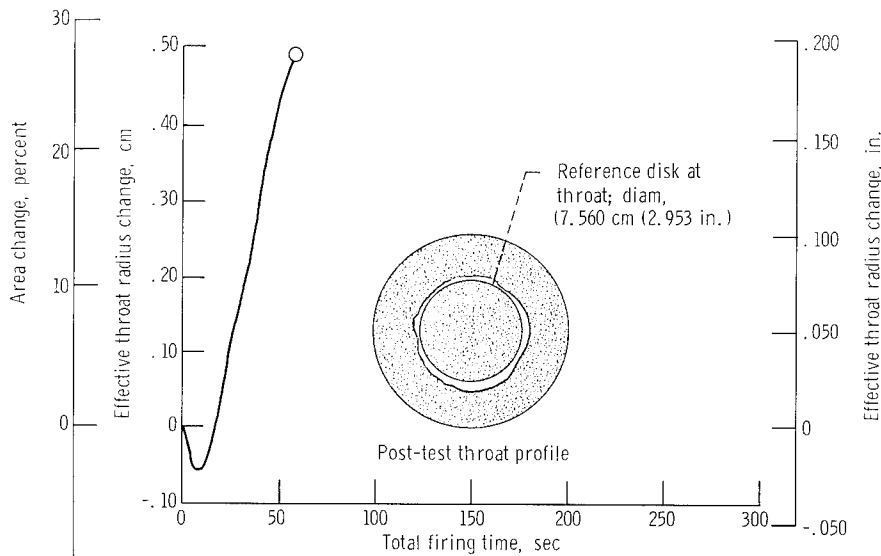
Figure 16. - Ablative erosion of silica phenolic (MX2646) chamber nozzle. Injector 2.

The efficiency measured for injector 2 is shown in figure 15. The ηC^* was 1.5 percent higher than that of injector 1. Test firing with MX2646 ablative material produced the results illustrated in figure 16. Although steady-state erosion was still high, there was a more uniform erosion pattern. Therefore, it was decided to continue testing injector 2. The next step was to test a throat insert for erosion resistance over a complete 700-second duty cycle.

In previous 700-second testing of throat inserts (ref. 4), ablative chamber durability was a problem. Erosion of the ablative chamber allowed silica to flow over the insert which action in itself caused melting and erosion of the insert. Ablative chamber erosion also could allow combustion gases to flow behind the throat insert. For these reasons, a series of firings was accomplished with a silica-phenolic ablative chamber to determine chamber durability with injector 2. The ablative chamber of the previous firing (fig. 16) was used but the eroded ablative nozzle was replaced by a water-cooled nozzle. The results after 433 seconds total firing are shown on figure 17. The outer ablative sleeve

24

Flow

C-68-4249
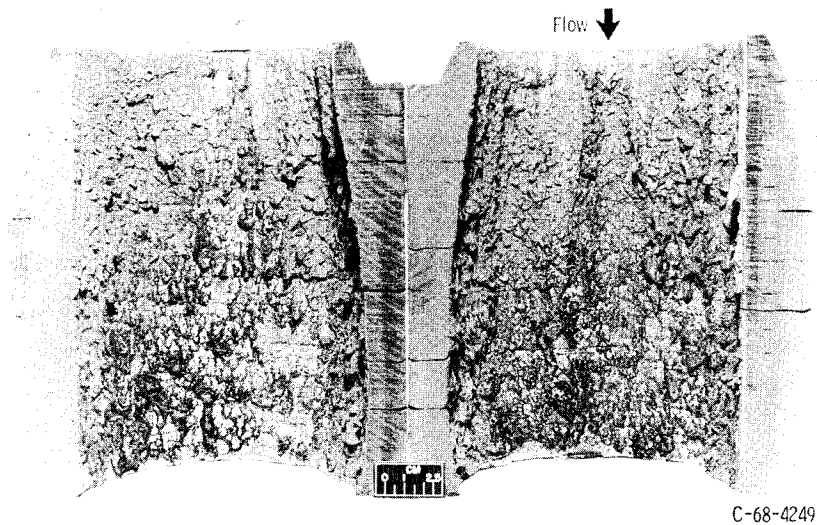
Figure 17. – Silica phenolic chamber section after 433-second total firing time. Injector 2; chamber pressure, 690 kN/m^2 (100 psia); oxidant-to-fuel ratio, 2.0.

Ablative throat erosion (from fig. 15)
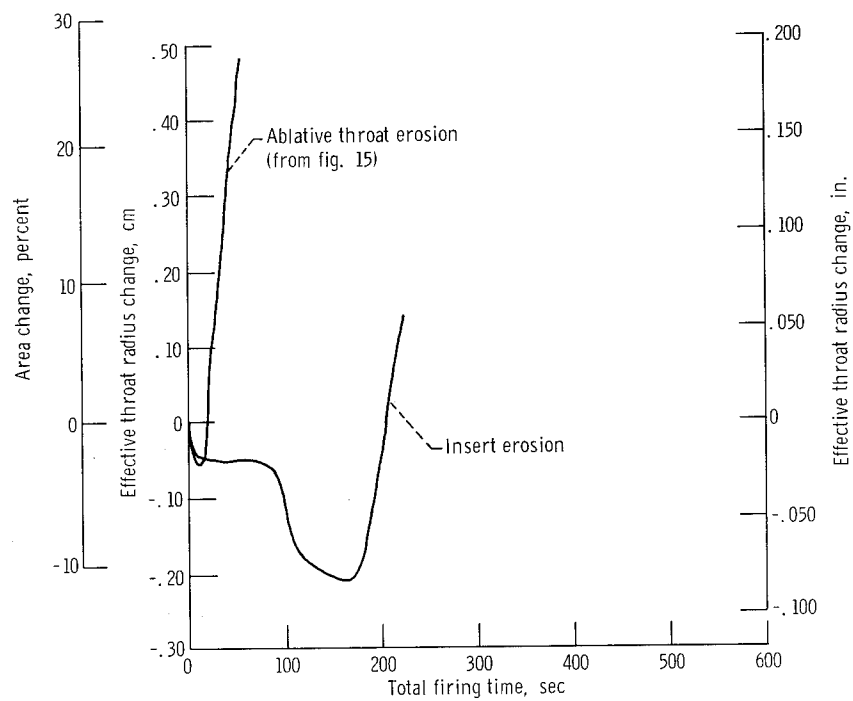
Insert erosion

Figure 18. – Erosion results for zirconia insert (cast, mixed grain) with injector 2.

25

is not shown. The severely eroded ablative was not adequate. A JTA graphite chamber liner was used for 700-second firing durations.

A cast, mixed-grain-size zirconia (Zircoa proprietary designation 1027-28D) throat insert was used with the JTA graphite chamber liner. The insert choice was based upon results in reference 4. The design was that of figure 11(a). The results of a 220-second duration test are given in figure 18. The apparent throat radius decrease at 100 seconds was probably caused by a high flow rate of decomposition products and small particles from the upstream portion of the insert and liner rather than any geometrical area change. This is followed by rapid throat erosion, and the test firing was aborted. Inspection of the chamber showed severe erosion of the insert and liner. Chamber liner erosion was
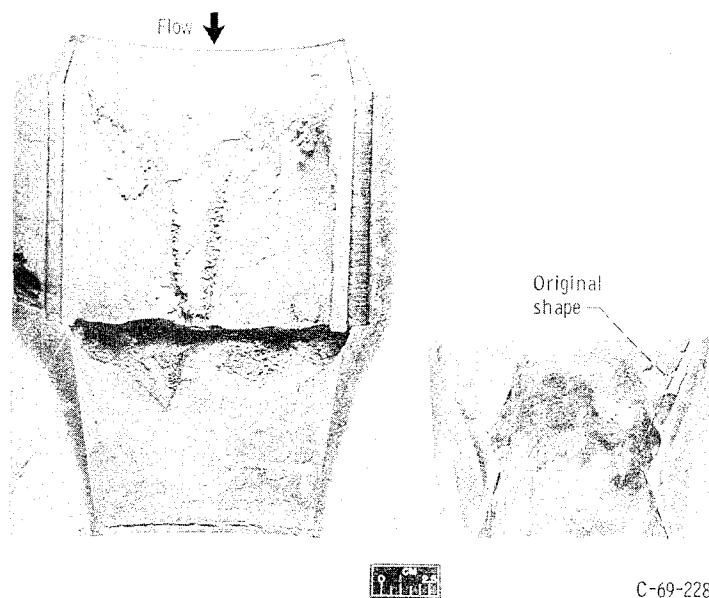
Figure 19. - Zirconia insert (cast mixed grain) after 227-second total firing time. Injector 2; chamber pressure, 690 kN/m^2 (100 psia); oxidant-to-fuel ratio, 2.0.

due to oxidation. Insert erosion was due to structural failure and melting. Figure 19 illustrates the post-test thrust chamber condition. It was concluded that the combustion gas temperature applied to the throat insert was too high for ZrO_2 which was among the better materials tested in reference 4.

Therefore, injector 2 was modified to provide a lower combustion temperature environment similar to that of reference 4 while still maintaining high ηC^* if possible. Injector 2 was modified by enlarging the outer fuel hole diameters in the 36 outer elements from 0.046 to 0.061 centimeter (0.018 to 0.024 in.) (see fig. 5(a)). This resulted in a peripheral zone mixture ratio of 1.22 with an attendant decrease in zone combustion gas temperature. The modification also changed the injector velocity ratio from 0.67 to 0.96.
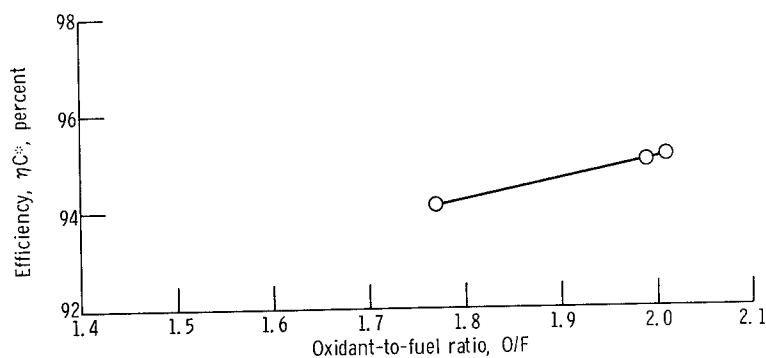
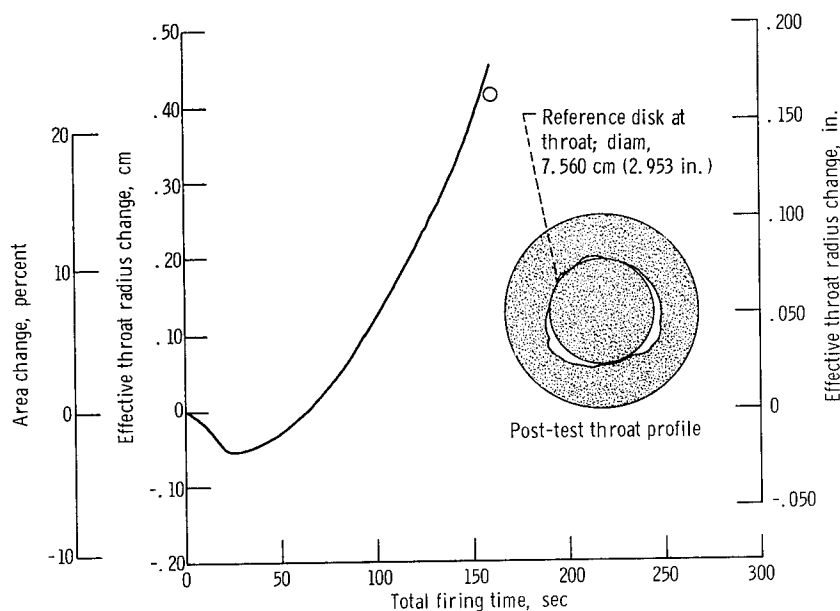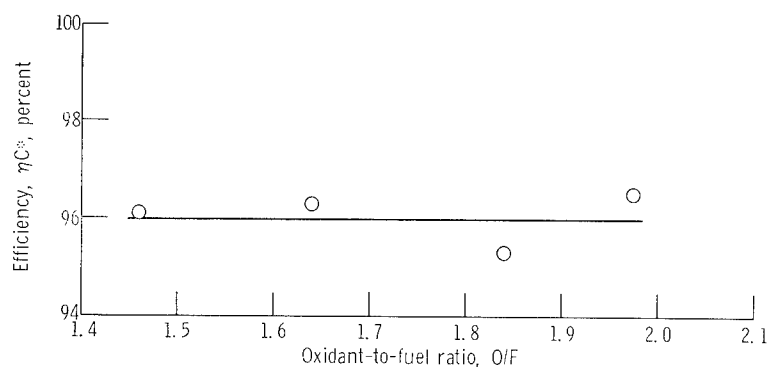Figure 20. - Injector 2A combustion performance.

Figure 21. - Erosion results for silica phenolic (MX2646) ablative with injector 2A.

The ηC^* values measured for injector 2A are given in figure 20. The efficiency was 3 percent below that for the unmodified injector. Erosion results with MX2646 ablative material illustrate (fig. 21) a lower steady-state erosion rate but pronounced gouging of the ablative throat.

Because of the lower than desired efficiency and more pronounced gouging character-istics, another injector modification was performed (see fig. 5(b)). The 36 outer ele-ments were arranged radially to make fans parallel to the wall for better ablative compat-ibility. The fuel hole diameters on 30 of the elements were reduced from 0.061 to 0.057 centimeter (0.024 to 0.0225 in.) diameter for lower V_{ox}/V_f (0.96 to 0.80) to provide higher performance. The design mixture ratio in the outer zone was changed to 1.4, which would raise the peripheral zone combustion temperature but not as high as the tem-

27
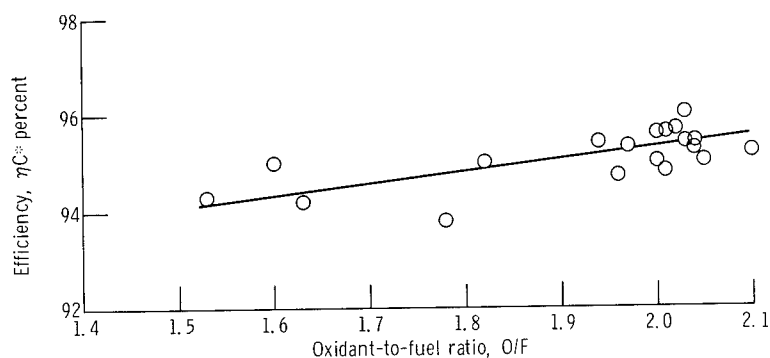
Figure 22. - Injector 2B combustion performance.
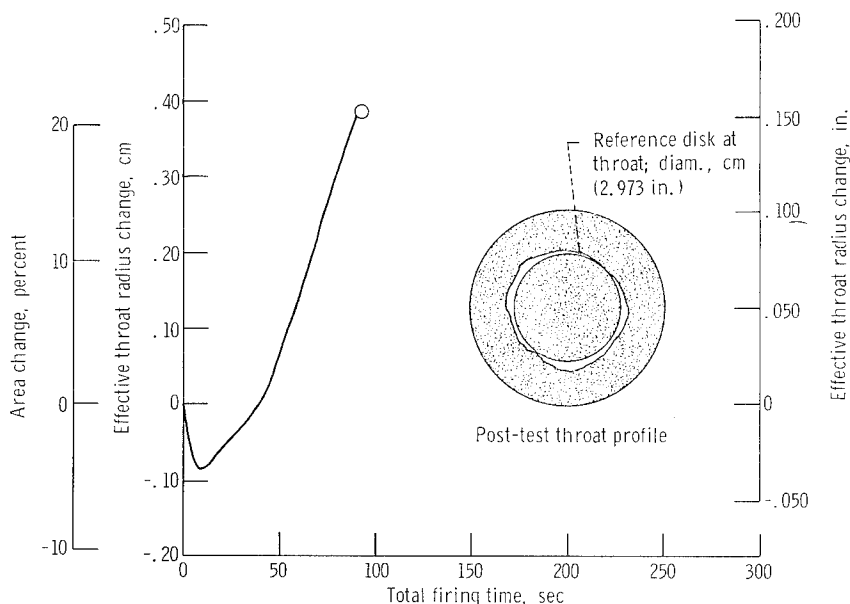
Figure 23. - Erosion results for silica phenolic (MX2646) ablative with injector 2B.

perature of the unmodified injector. Figure 22 shows the ηC^* for injector 2B - a level considered satisfactory.

The ablative erosion results are on figure 23. The steady-state erosion rate and uniformity were reasonably good but a further improvement in ablative compatibility was sought by changing to injector 2C as illustrated on figure 5(c). Each fuel hole on the outside of each outer element was replaced by two impinging fuel holes in order to provide more uniform coverage of the oxidant jet with fuel at a design mixture ratio of 1.31. The peripheral zone combustion temperature would be between the zone temperatures of the previous modifications. The outer elements were designed for axial or slightly inward momentum. The exact element layout (fig. 5(c)) was intended to blanket the oxidant with fuel when the jet spreading angles of 5° were included. Specific element dimensions

28

Figure 24. - Injector 2C combustion performance.
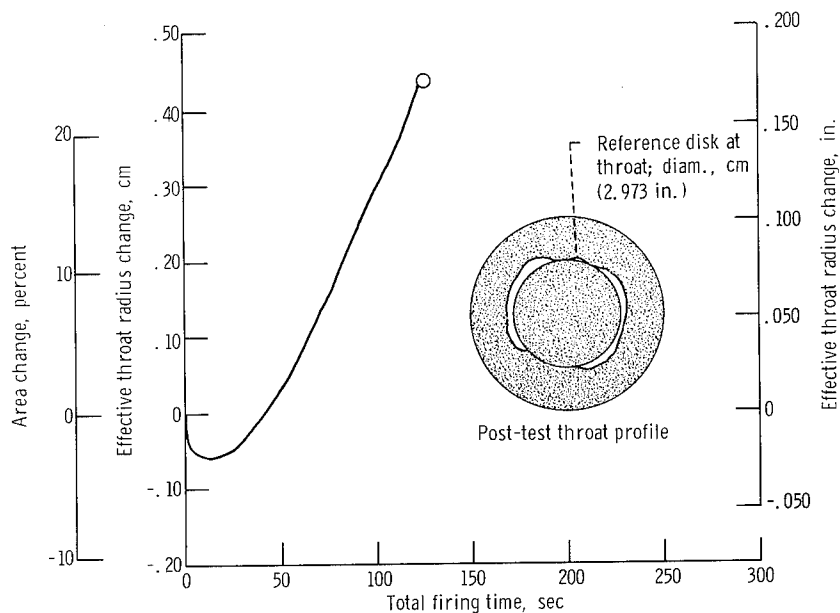
Figure 25. - Erosion results for silica phenolic ablative with injector 2C.

(table on fig. 5(c)) were different because the holes were restricted in position and angle by the supply manifold location. The ηC^* values for injector 2C are plotted in figure 24. The nominal efficiency was 95.3 percent at the design O/F of 2.0 with a standard deviation of ±0.4 percent on the ηC^* values.

Ablative throat erosion results are given on figure 25. A definite squareness is seen at the throat, however, the steady-state erosion rate of 0.0053 centimeter per second (0.0021 in./sec) was considered acceptable.

Table II presents the ηC^* results of the five injectors tested along with equivalent ablative erosion results. Injector 2C was slightly more efficient than injector 2A with an attendant higher erosion rate. Both 2A and 2C significantly decreased the ablative erosion rate below that of injector 2 with a 2.0 to 2.6 percent loss in efficiency. Since

TABLE II. – ABLATIVE-INJECTOR PERFORMANCE

Injector	Efficiency, ηC^*, % theoretical equilibrium	Time to start erosion, sec	Steady-state erosion rates	
			cm sec	in. sec
1	95.9	12	0.0127	0.0050
2	97.6	17	.0132	.0052
2A	95.0	64	.0048	.0019
2B	96.0	39	.0076	.0030
2C	95.3	42	.0053	.0021

C-68-4091
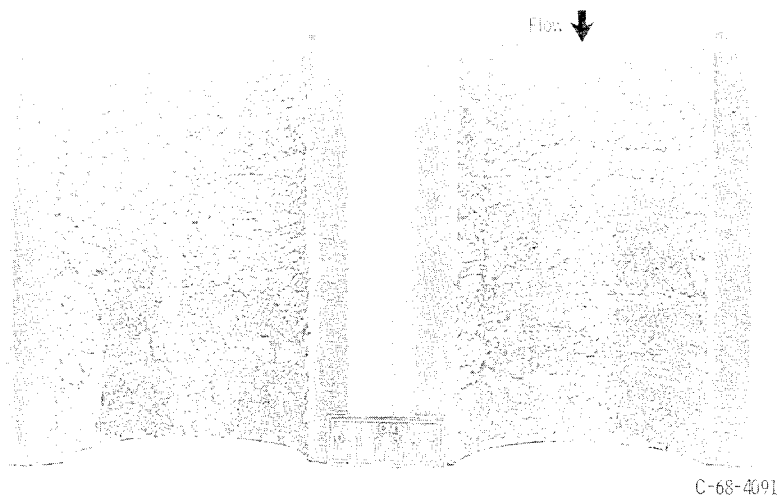
Figure 26. – Silica-phenolic chamber section after 428-second total firing time. Injector 2C; chamber pressure, 690 kN/m^2 (100 psia); oxidant-to-fuel ratio, 2.0.

further modifications would have been physically difficult, as well as unlikely to significantly improve the ablation characteristics, it was decided to proceed with throat insert testing using injector 2C.

The next step was to recheck ablative chamber erosion during long firings. The same chamber used for the firing shown in figure 25 was tested with the water-cooled nozzle for an additional 300 seconds. The results are illustrated on figure 26. Long-term ablative compatibility was considerably better with injector 2C (fig. 25) than with

injector 2 (fig. 16). Nevertheless, it was concluded that a chamber liner would still be required to prevent excessive chamber erosion for a total firing duration of 700 seconds. The remainder of the inserts tested had the liner-insert configuration of figure 11(a).

Throat Insert Evaluation

Having demonstrated that a throat insert is required to minimize erosion at C^* efficiencies above 95 percent, the following types of throat inserts were tested: oxides including ZrO_2 and BeO, and a composite of HfC, SiC, and graphite. Various construction techniques used with oxides include segmenting and reinforcing with W-Re wires. A summary of the designs and test results is given in table III.

TABLE III. - THROAT INSERT TEST SUMMARY

| Insert material	Injector	Total firing cycles	Total firing time, sec	Throat area change, percent	Failure mode
Cast mixed grain ZrO_2 (1027-28D)	2	1	220	+8	Structural thermal
Cast mixed grain ZrO_2 (1027-28D)	2C	6	400	+2	Structural
HfC, SiC, C (JT0992)	2C	1	138	+5	Oxidation
Segmented BeO	2C	3	340	-4	Structural
ZrO_2 (F410) Reinforced with 5 vol. % 0.0089-cm (0.0035-in.) diam. W-Re wires	2C	7	640	-4	Structural
ZrO_2, MgO Stabilized reinforced with 7 vol. % 0.005-cm (0.002 in.) diam. W-Re wires	2C	7	700	-6	None
ZrO_2, MgO Stabilized reinforced with 7 vol. % 0.0089-cm (0.0035-in.) diam. W-Re wires	2C	7	700	-2	None
ZrO_2 MgO Stabilized	2C	2	21	+48	Structural
ZrO_2 (F410) Segmented reinforced with 5 vol. % 0.0089-cm (0.0035-in.) diam. W-Re wires	2C	7	700	-7	None
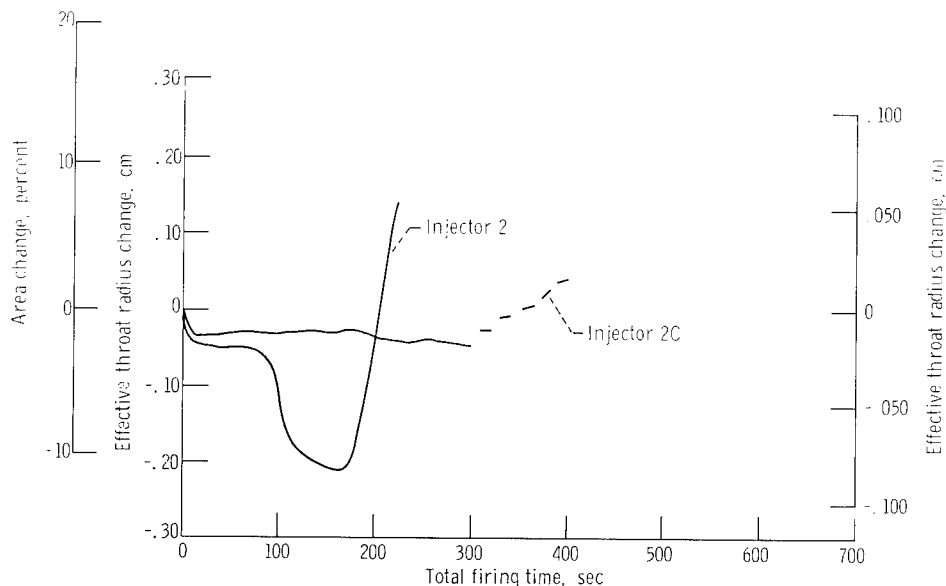
Figure 27. – Erosion results of zirconia insert (cast, mixed grain) with injector 2C.

A cast, mixed-grain-size zirconia insert (Zircoa proprietary designation 1027-28D), identical to that tested with injector 2, was selected for the initial tests with injector 2C. The erosion results are given on figure 27. A significant improvement in insert erosion is noted compared to the results with injector 2. The injector modification was successful in preventing melting of the ZrO_2 throat insert. After the initial 300-second firing, some minor axial and circumferential cracks were evident without loss of material. During the five 20-second firings, loss of material due to spalling occurred as illustrated in figure 28. Although throat erosion was low, severe loss of material upstream of the throat was considered indicative of insert failure so that testing was discontinued. This material performed better in the 3.05-centimeter (1.2-in.) throat diameter of reference 4 where 700 seconds of testing produced cracking but no significant loss of material.

The next insert material selected for testing was JT0992 – a HfC-SiC-graphite composite material that performed fairly well in the smaller scale inserts. The key to success for this material was the formation and retention of a protective oxide layer during engine firing. The test firing of this insert was ended after 138 seconds because of a high rate of erosion (fig. 29). The post-test condition of the insert is illustrated on figure 30. Traces of the oxide formed are evident as well as burn-through of the insert due to structural failure. The penalty for structural failure was dramatically illustrated. The amount of graphite in the composite was not sufficient to prevent structural failure. Neither were the oxides formed from the carbides sufficiently adherent to prevent further oxidation.

An insert constructed of BeO segments was tested next. Both axial and circumfer-
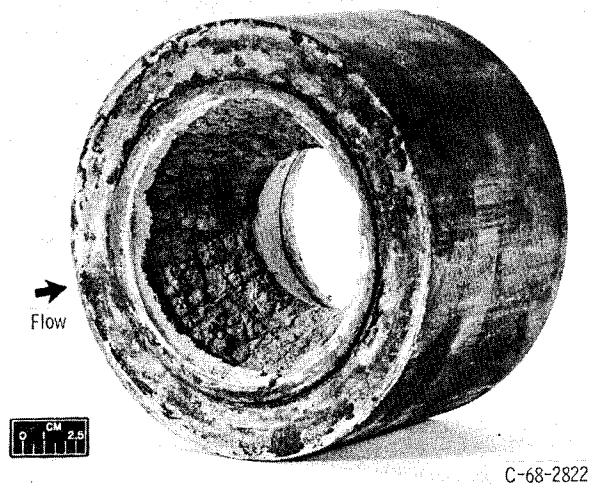
Figure 28. – Zirconia insert (cast mixed grain) after 401-second total firing time. Injector 2C; chamber pressure, 690 kN/m^2 (100 psia); oxidant-to-fuel ratio, 2.0.
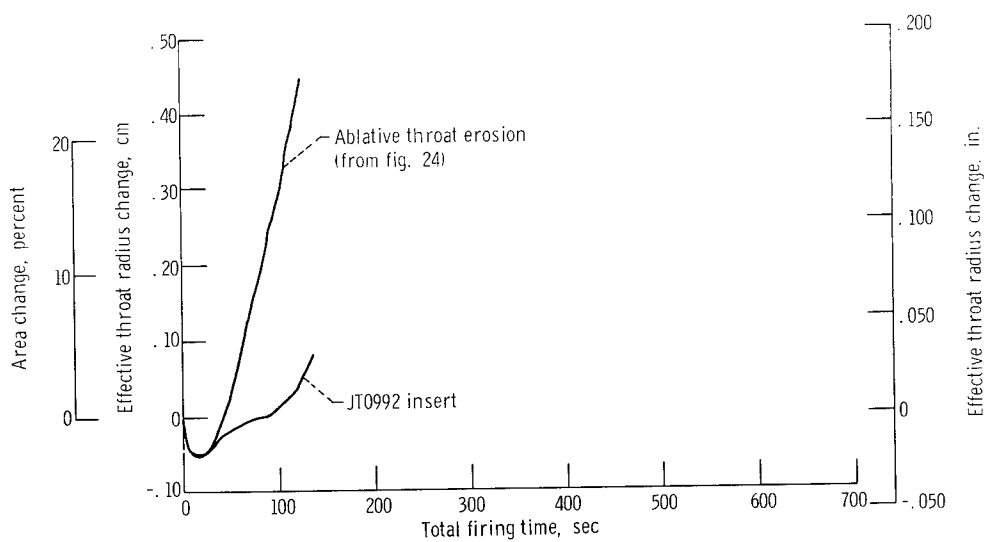

Figure 29. – Erosion results for JT0992 insert (composite of HfC, SiC, and graphite) with injector 2C.
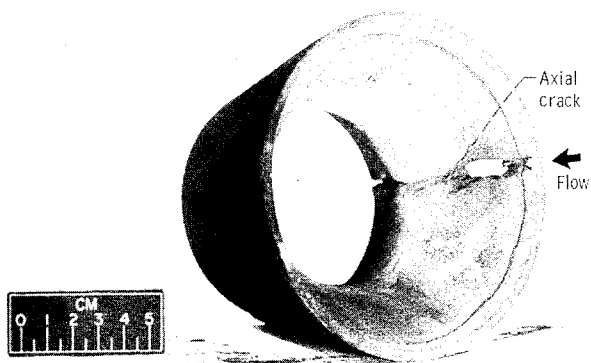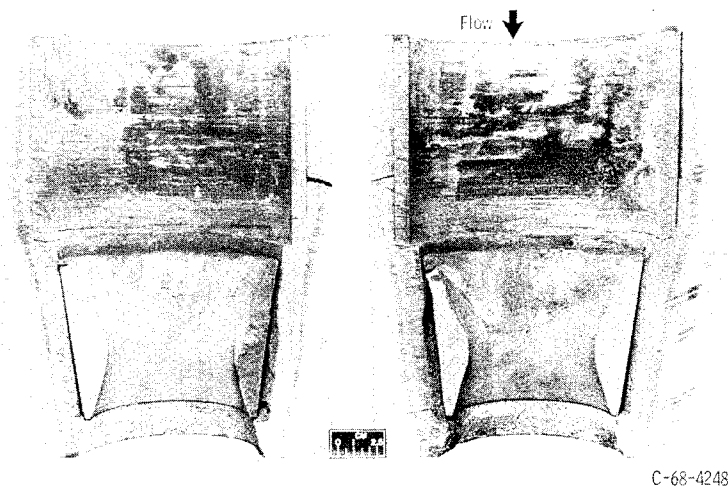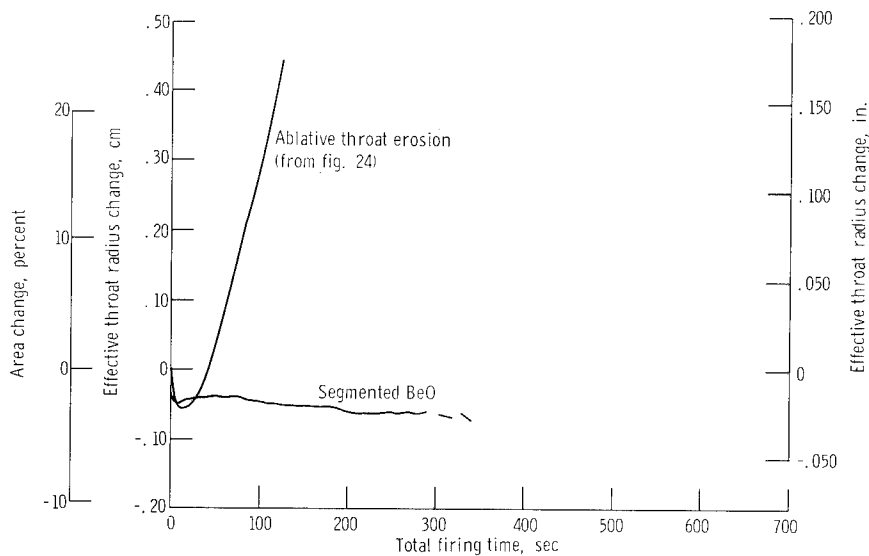
C-68-4248

Axial
crack

Flow

C-68-3167

Figure 30. - JTO992 insert after 138-second total firing time. Injector 2C; chamber pressure, 690 kN/m^2 (100 psia); oxidant-to-fuel ratio, 2.0.

Figure 31. - Erosion results for segmented beryllium oxide (BeO) insert with injector 2C.

ential segments were used and the segments were contained in a 0.625-centimeter (1/4-in.) thick BeO sleeve to prevent gas leakage. Figure 11(b) shows insert construction details. Insert throat radius change from hot firing with injector 2C is shown in figure 31. After the initial 300-second firing, some loss of material at the segment interfaces was evident. The throat plane was not affected and the segments were not badly cracked. Following two additional 20-second firings, however, much cracking and loss of material upstream of the throat was observed (see fig. 32). Although no throat erosion had occurred, it was felt that total failure was imminent, and testing was stopped to prevent excessive scattering of the BeO. It is evident that the segmented construction used here does not prevent thermal stress failure of BeO.

A material combination intended to combat thermal stress failure was an F410 CaO-MgO stabilized zirconia matrix reinforced with 5 volume percent tungsten-rhenium wires (diam., 0.0089 cm or 0.0035 in.). This material had been tested in a smaller throat size (ref. 4), and it prevented throat erosion over the desired duty cycle. Cracking was found in the smaller scale tests, however, so that testing in the larger size was required to determine whether significant loss of material would result. A heat-transfer analysis predicted the maximum thermal gradient across the insert to be 2050 K (3700° R) at 18 seconds firing time. Maximum char depth in the ablative holder was calculated to be only 0.625 centimeter (0.25 in.) after 300 seconds of firing. The design appeared to be thermally adequate for the 700-second duty cycle.
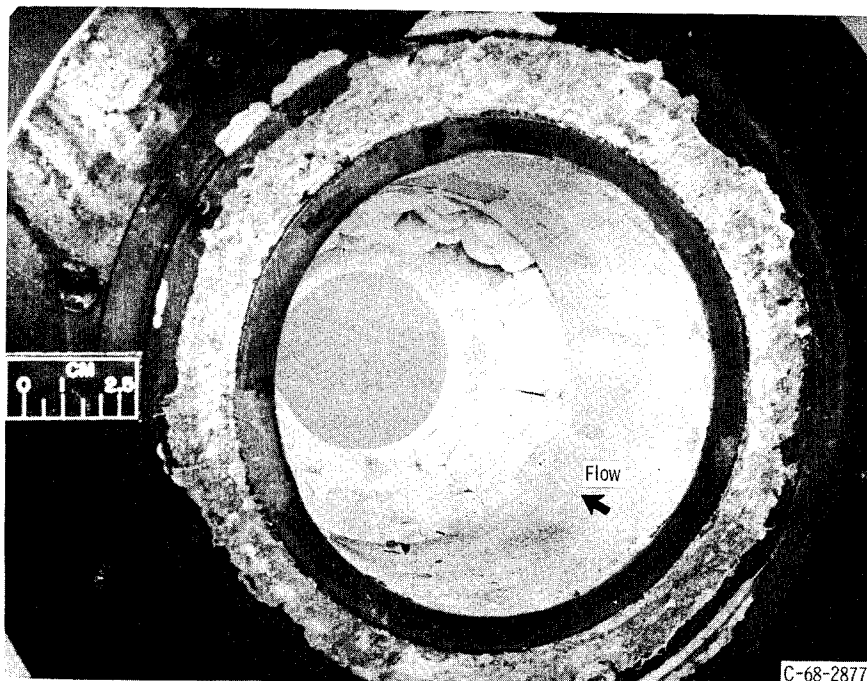

Figure 32. - Segmented beryllium oxide insert after 340-second total firing time. Injector 2C; chamber pressure, 690 kN/m^2 (100 psia); oxidant-to-fuel ratio, 2.0.

Assuming a temperature gradient of 2050 K (3700° R), stress analysis predicted a maximum hoop stress of 214 MN/m² (31 000 psi) tension and maximum axial stress of 62 MN/m² (9500 psi) tension on the insert outside surface after 40 seconds of firing. The ultimate tensile strength of the insert material was estimated to be 69 MN/m² (10 000 psi). Structural failure was thus predicted, but it was hoped that many small microcracks would form to relieve the overall stress level before macrocracks occurred. It was also hoped that cracking would not lead to significant loss of material.
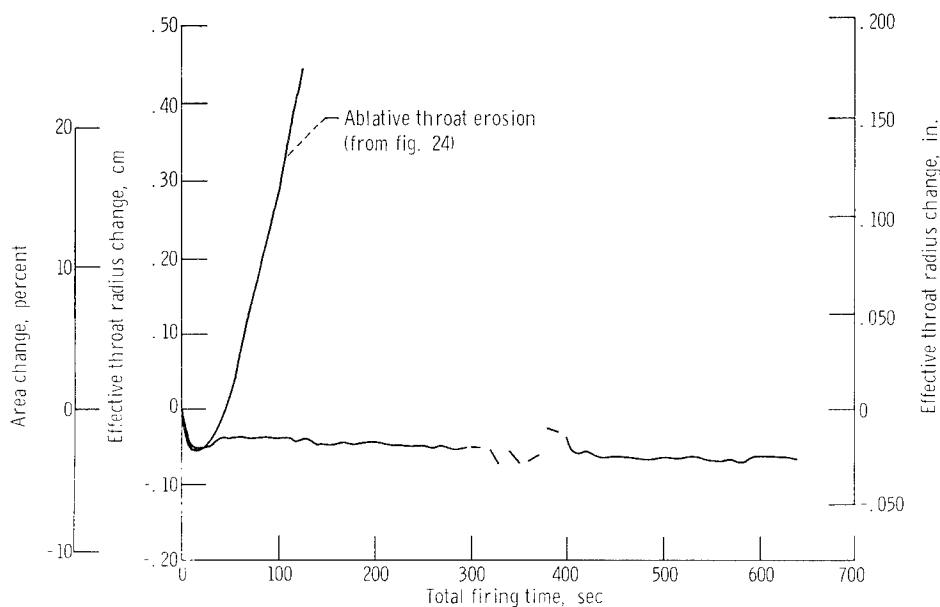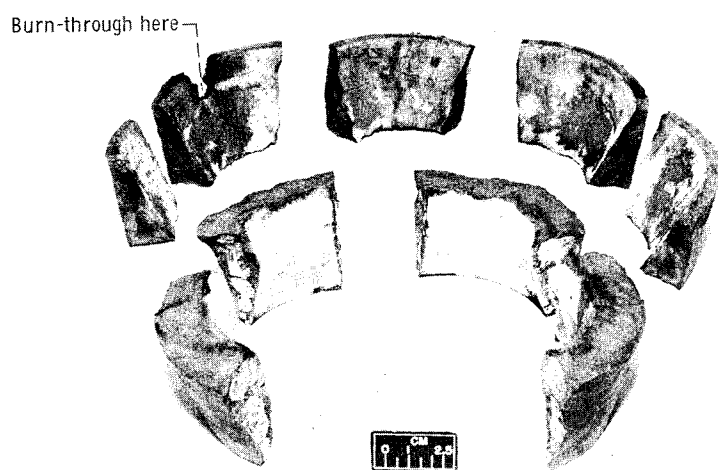

Figure 33. - Erosion results for zirconia (F 410) insert reinforced with 5-volume-percent tungsten-rhenium wires. Wire diameter, 0.0089 centimeters (0.0035 in.). Injector 2C.

Throat radius change is shown on figure 33 for the total firing time. Cracking of the insert was observed after the initial 300-second firing (see fig. 34(a)). The cracks were not completely through the insert, however. The five 20-second firings caused no erosion but after 240 seconds of the final firing, a combustion gas leak occurred because of the loss of insert material, and the firing was terminated. Figure 34(b) shows the insert after the final test. Thermal stress cracking led to loss of insert material which resulted in chamber burnthrough. The possibility of catastrophic failure due to uncontrolled cracking was dramatically illustrated.

Based on the results of reference 4, a contract (ref. 8) was let to design and fabricate reinforced oxide throat inserts for the 7.62-centimeter (3.0-in.) throat diameter engine. A magnesia stabilized zirconia matrix with 7 volume percent tungsten-rhenium wire reinforcement was selected for the rocket engine firing evaluation based on the work of reference 8. The reinforcing wires were 0.005-centimeter (0.002-in.) diameter
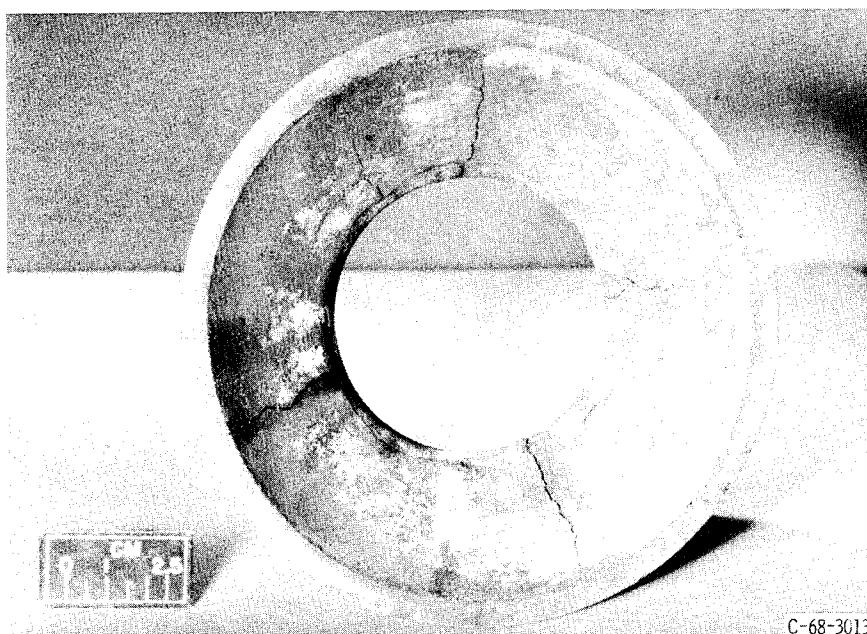
(a) After 300-second firing time.

(b) After 650-second total firing time.

Figure 34. - Zirconia (F410) insert reinforced with 5-volume-percent tungsten-rhenium wire (diam, 0.0089 cm or 0.0035 in.). Injector 2C; chamber pressure, 690 kN/m^2 (100 psia); oxidant-to-fuel ratio, 2.0.
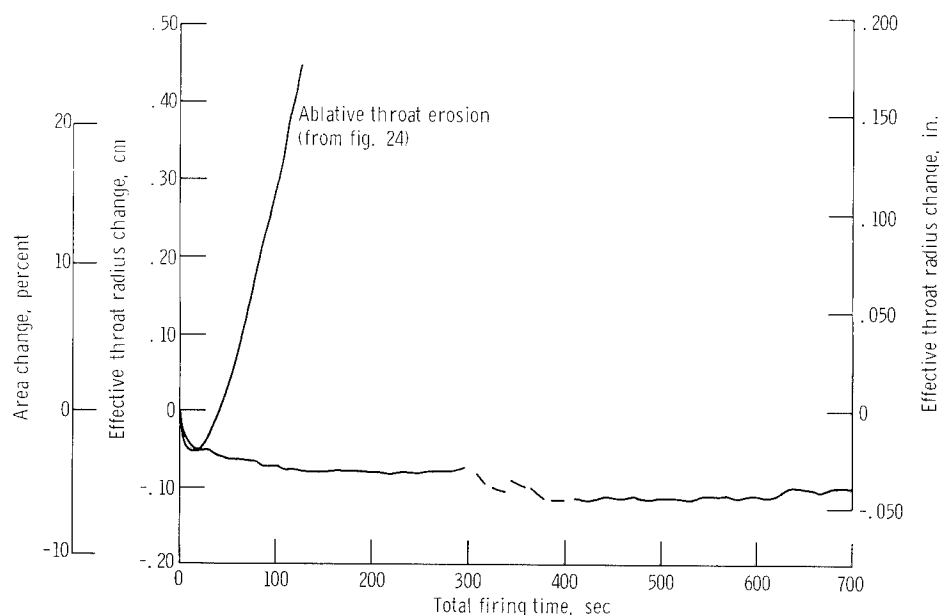
Figure 35. – Erosion results for zirconia insert reinforced with 7-volume-percent tungsten-rhenium wires (diam, 0.005 cm or 0.002 in.). Injector 2C.

rather than the 0.0089-centimeter (0.0035-in.) diameter wires used previously. The erosion data during the firing are presented in figure 35. A throat area decrease of about 6 percent was measured over the total duty cycle. Inspection of the insert following testing revealed surface spallation and roughening along with cracking on the outside surface. (See figure 36 for post-test views of the insert.) The throat area decrease was most likely caused by phase change (volume increase) of the zirconia matrix material.

Under the contract of reference 8 and based on engine firing results, an attempt to further improve the insert surface characteristics and structural integrity was made. The magnesia stabilized zirconia matrix was reinforced with 7-volume-percent tungsten - rhenium wires (wire diam., 0.0089 cm or 0.0035 in.). The intent was to approach the surface characteristics of the F410 zirconia reinforced with the 0.0089-centimeter (0.0035-in.) diameter wires, while decreasing the cracking tendencies by maintaining 7-volume-percent reinforcement. The throat erosion results for the entire hot-firing sequence are presented in figure 37. A net throat area decrease of 2 percent was measured compared to 6 percent area decrease for the insert containing 0.005-centimeter (0.002-in.) diameter wires. Post-test inspection of the insert revealed a flaky porous surface with numerous cracks in the substructure but not separation of the parts (see fig. 38). Both of the magnesia stabilized zirconia inserts reinforced with the 0.005- and the 0.0089-centimeter (0.002- and 0.0035-in.) diameter wire performed reasonably well, however.

Under contract (ref. 8), an unreinforced zirconia nozzle was also fabricated to make a qualitative comparison of the influence of the wire reinforcement on the insert structure. Manufacture of a sound insert using exactly the same techniques as were used for the re-
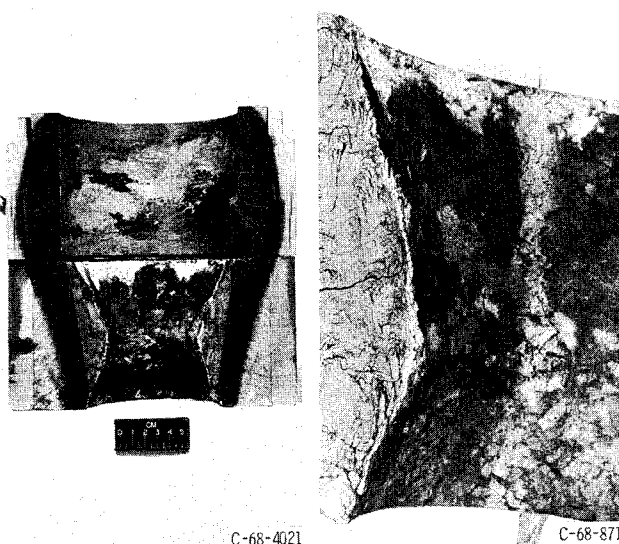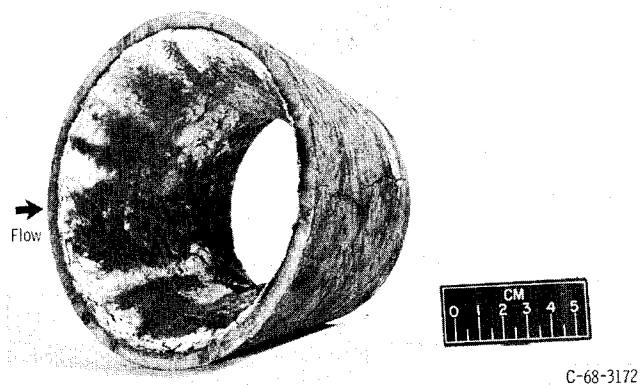
Figure 36. - Zirconia insert reinforced with 7-volume-percent tungsten-rhenium wires (diam, 0.005 cm or 0.002 in.) after 700-second total firing time. Injector 2C; chamber pressure, 690 kN/m^2 (100 psia); oxidant-to-fuel ratio, 2.0.
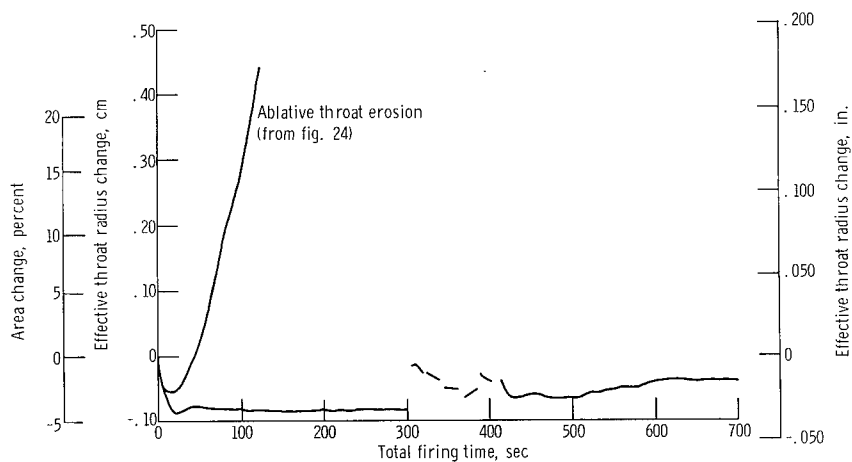

Figure 37. - Erosion results for zirconia (ZrO$_2$) insert reinforced with 7-volume-percent tungsten-rhenium wires (diam, 0.0089 cm or 0.0035 in.). Injector 2C.

Figure 38. – Zirconia (ZrO_2) insert reinforced with 7-volume-percent tungsten-rhenium wires (diam, 0.0089 cm or 0.0035 in.) after 700-second total firing time. Injector 2C; chamber pressure, 690 kN/m^2 (100 psia); oxidant-to-fuel ratio, 2.0.
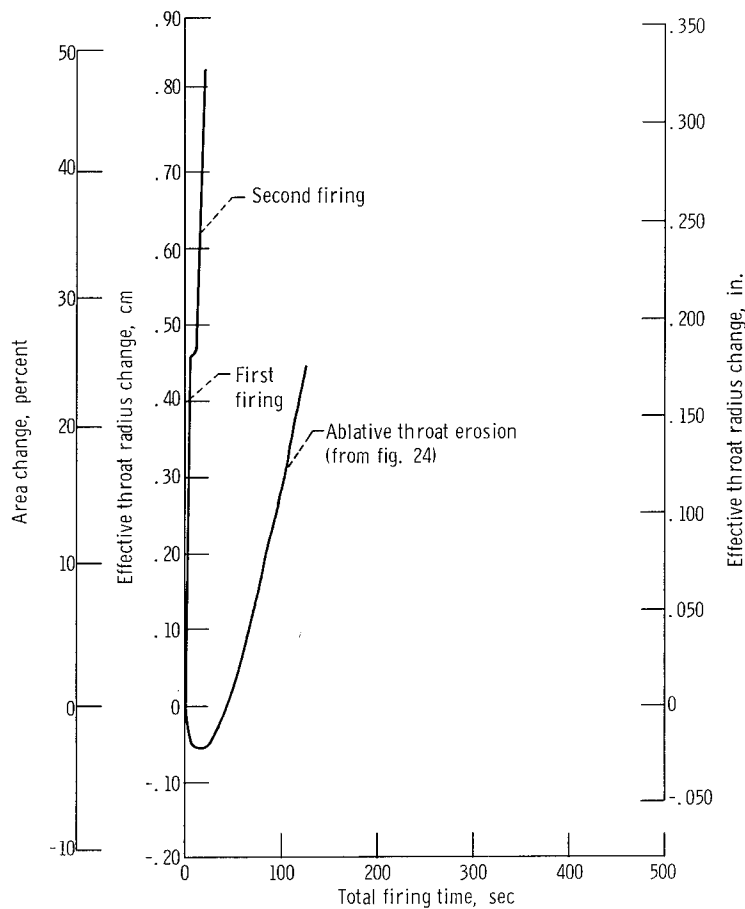
Figure 39. - Erosion results for unreinforced zirconia (ZrO$_2$) insert. Injector 2C.

inforced insert was not possible. Sintering the pressed insert at both 139 K per hour (250° R/hr) and 93 K per hour (167° R/hr) resulted in severely cracked inserts. As a result, a mixture of coarse and fine particles was required with considerably slower heating and cooling rates. The finished insert was tested twice with very rapid erosion rates as shown in figure 39. The failure mechanism was spallation and loss of small particles due to thermal shock. The mechanism and rate were similar to results with the 90 percent dense yttria stabilized inserts of reference 4. It is possible that with the use of different grain sizes, other stabilizers, and more refined processing techniques the unreinforced insert might have performed more satisfactorily (see fig. 27). The effect of the reinforcing wires was, nevertheless, dramatically illustrated. However, the surface condition of the unreinforced magnesia stabilized insert was similar to that of the reinforced insert. The flaky, nonadherent surface structure suggests that a better zirconia matrix material could be found that would more closely approach the surface results for the F410 material but still eliminate major cracking problems.

A combination of techniques was used in an attempt to solve the previous insert prob-

lems. A zirconia material was selected to prevent oxidation. Specifically, the F410 material reinforced with 5 volume percent tungsten-rhenium wires (0.0089 cm or 0.0035 in.) was chosen for its good surface protection during the previous testing. The insert was segmented to prevent catastrophic structural failure, and the reinforcement was used to improve the structural properties of each segment. The construction of the segmented design is illustrated in figure 11(c). The insert was sintered and pressed in a single billet and then cut into segments. Since the insert-liner materials were essentially the same as those tested previously (see fig. 11(a)), no change in the temperature gradient of 2050 K (3700° R) was expected. Axial segmenting was used to prevent axial stress failure by reducing axial stress. Radial segments were designed to reduce hoop stress below the ultimate value to solve the cracking failure found in the monolithic insert tested previously. Since hoop stress on the outer surface of the insert was no longer a problem, the compressive stress on the segment inside surface was evaluated. The amount of stress in each segment depends on the amount of restraint given the segments. For the nonsegmented insert, a compressive stress of about 255 MN/m^2 (37 000 psi) was predicted at about 5 seconds firing time. A completely restrained segmented design was calculated to have 276 MN/m^2 (40 000 psi) compression. A completely unrestrained segmented design was calculated to have 200 MN/m^2 (29 000 psi) compression. With the 0.010-centimeter (0.004-in.) bond line between segments, the design was expected to more nearly approach the unrestrained case. At any rate, all stresses were below the ultimate compressive stress of 690 MN/m^2 (100 000 psi). The segmented design was intended to prevent uncontrolled cracking leading to loss of insert material.

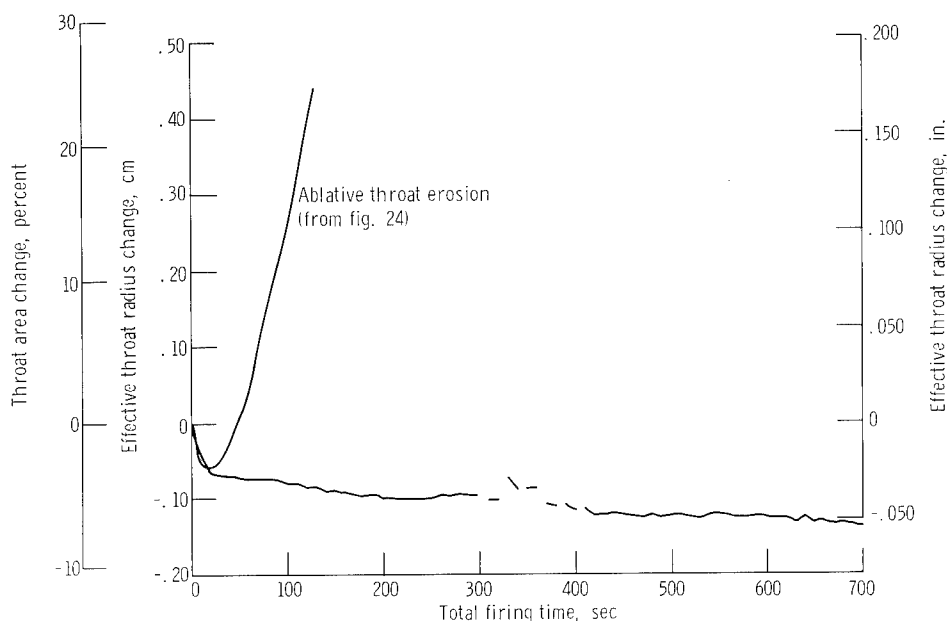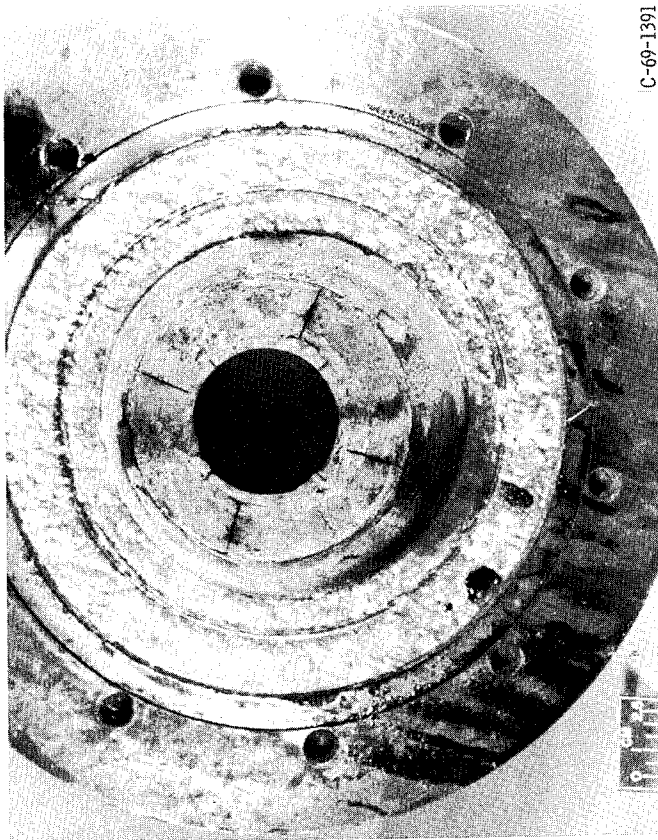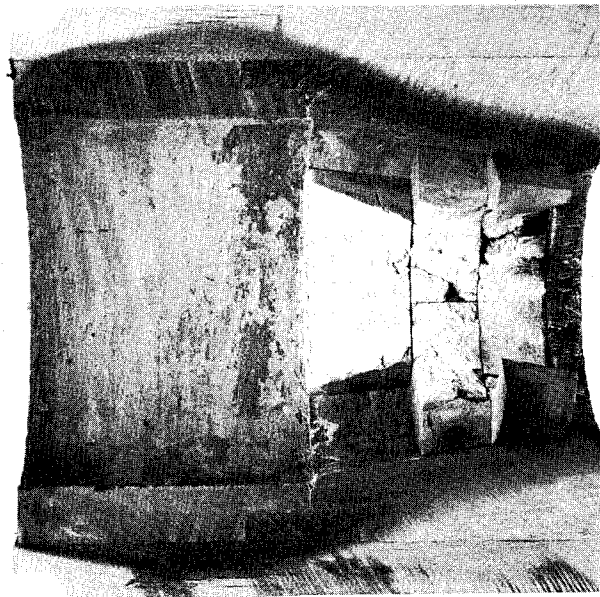The throat radius change data are presented in figure 40. The entire duty cycle was
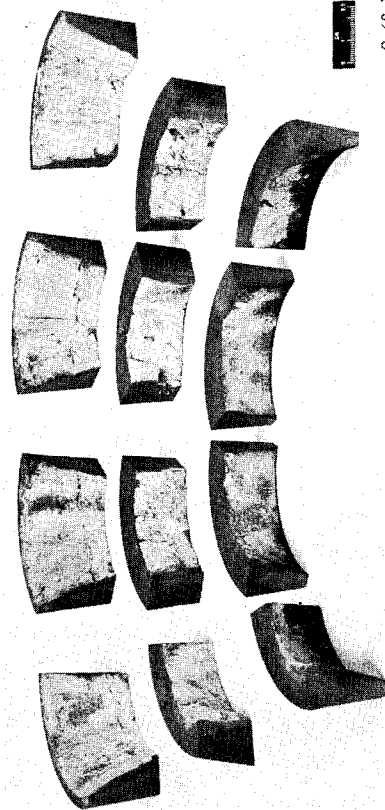

Figure 40. - Erosion results for segmented zirconia (F 410) insert reinforced with 5-volume-percent tungsten-rhenium wires (diam, 0.0089 cm or 0.0035 in.). Injector 2C.

Figure 41. - Segmented zirconia insert reinforced with 5-volume-percent tungsten-rhenium wires (diam, 0.0089 cm 0r 0.0035 in.) after 700-second total firing time. Injector 2C; chamber pressure, 690 kN/m² (100 psia); oxidant-to-fuel ratio, 2.6.
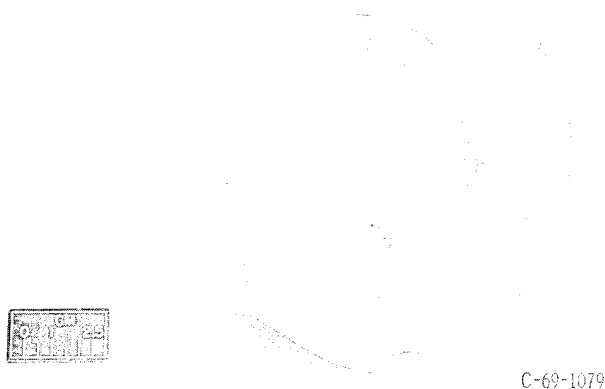
C-69-1786

C-69-1391

C-69-1785

Figure 42. - Segmented zirconia insert reinforced with 5-volume-percent
tungsten-rhenium wires (diam, 0.0089 cm or 0.0035 in.) before test.

C-69-1079

run with a throat area decrease of 7 percent. Inspection of the insert following testing revealed some cracking and loss of material, but none of the segments was completely broken (see fig. 41). Cracks were only associated with void areas formed during manufacture of the original billet (see fig. 42). These void areas could be eliminated by fabricating single segments and discarding those of questionable quality prior to assembly of the throat insert. The insert had been fabricated as one billet in this case to avoid the cost of new tooling. The concept of constructing a segmented throat insert was proven although material selection still plays a major role in the design process.

SUMMARY OF RESULTS

During the injector development phase of the program, five injector configurations were tested with ablative thrust chambers. Several hard throat inserts were then tested using the best injector to demonstrate throat erosion control. Nominal engine operating conditions were 690 kN/m^2 (100 psia) chamber pressure and an oxidant-to-fuel ratio of 2.0 using nitrogen tetroxide oxidizer with a 50-percent blend of unsymmetrical dimethyl hydrazine and hydrazine fuel. The engine throat diameter was 7.62 centimeters (3.0 in.), which provided 4450 newtons (1000 lbf) with a sea level expansion area ratio of 2.0. An arbitrary duty cycle of one 300-second firing, five 20-second firings, and one 300-second firing was selected to demonstrate long-term firing with restart capability.

The following conclusions were reached:

1. Careful injector design is required to combine satisfactory combustion performance with uniform ablative erosion. Throat insert and combustion chamber longevity are also sensitive to injector performance and local mixture ratio. It is desirable to main-

44

tain boundary-layer temperatures below the melting point of the insert material chosen and to be sure that the injector is compatible with the selected chamber design. To the extent needed for the chosen duty cycle, all these problems were solved during the engine development.

2. A segmented design presents a solution to the structural failure problem associated with oxide materials. Materials must be selected and constructed with care, however, since a segmented beryllium oxide insert failed structurally during testing. A segmented insert of tungsten-rhenium wire reinforced zirconia provided both erosion resistance and structural integrity over the 700-second duty cycle. Further improvement could be made by molding each segment separately to insure uniform, void-free material.

3. Segmented throat inserts, carefully manufactured and constructed, probably offer the best method for controlling ablative erosion in engines with larger ($<$ 7.62 cm 3.0-in.) throat diameters requiring long firing duration missions with start-stop capability.

4. Nonsegmented magnesia stabilized zirconia inserts with tungsten-rhenium wire reinforcement provided satisfactory erosion resistance for 700 seconds but were subject to cracking. One solution to the cracking problem might be better optimization of the particular material combination.

5. Formation of uncontrolled macrocracks can lead to significant insert material loss and catastrophic failure of the rocket engine.

6. Oxides such as zirconia resist oxidation, but without reinforcement are subject to structural failure and loss of material due to surface spallation.

7. Materials subject to oxidation, such as JT0992, provide limited duration erosion resistance when used as throat inserts with the earth storable combustion products.

Lewis Research Center,
National Aeronautics and Space Administration,
Cleveland, Ohio, March 24, 1971,
731-12.

REFERENCES

1. Peterson, Donald A.: Experimental Evaluation of High-Purity-Silica Reinforced Ablative Composites as Nozzle Sections of 7.8-Inch (19.8-cm) Diameter Throat Storable-Propellant Rocket Engine. NASA TM X-1391, 1967.

2. Pavli, A. J.: Experimental Evaluation of Several Advanced Ablative Materials as Nozzle Sections of a Storable-Propellant Rocket Engine. NASA TM X-1559, 1968.

3. Peterson, Donald A.; Winter, Jerry M.; and Shinn, Arthur M., Jr.: Rocket Engine Evaluation of Erosion and Char as Functions of Fabric Orientation for Silica-Reinforced Nozzle Materials. NASA TM X-1721, 1969.

4. Winter, Jerry M.; and Peterson, Donald A.: Development of Improved Throat Inserts for Ablative Rocket Engines. NASA TN D-4964, 1968.

5. Winter, Jerry M.; and Peterson, Donald A.: Experimental Evaluation of 7.82-Inch (19.8-cm) Diameter Throat Inserts in a Storable-Propellant Rocket Engine. NASA TM X-1463, 1968.

6. Winter, Jerry M.; and Peterson, Donald A.: Evaluation of 7.8-Inch-Throat-Diameter Inserts and a Unique Cooling Concept in a Storable-Propellant Rocket Engine. NASA TM X-1756, 1969.

7. Aukerman, Carl A.; and Trout, Arthur M.: Experimental Rocket Performance of Apollo Storable Propellants in Engines with Large Area Ratio Nozzles. NASA TN D-3566, 1966.

8. Lally, F. T.; and Laverty, D. P.: Reinforced Oxide Throat Insert Development. Rep. ER-7326, TRW, Inc. (NASA CR-72573), Dec. 31, 1968.